Title

Synthesis and Self-Assembly of Well-Defined Block Copolypeptides via Controlled NCA Polymerization

Author

Deming, Timothy J

Publication Date

2013

DOI

10.1007/12_2013_234

Peer reviewed

Synthesis and self-assembly of well defined block copolypeptides via controlled NCA polymerization

Timothy J. Deming

Department of Bioengineering

University of California, Los Angeles

5121 Engineering 5

Los Angeles, CA 90095

ph. (310) 267-4450

Fax (310) 794-5956

e-mail: demingt@seas.ucla.edu

Table of Contents

Abstract This article summarizes advances in the synthesis of well-defined polypeptides and block copolypeptides. Traditional methods used to polymerize α-amino acid-N-carboxyanhydrides (NCAs) are described, and limitations in the utility of these systems for the preparation of polypeptides are discussed. Improved initiators and methods are also discussed that allow polypeptide synthesis with good control over chain length, chain length distribution, and chain-end functionality. Using these methods, block and random copolypeptides of controlled dimensions (including: molecular weight, sequence, composition, and molecular weight distribution) can now be prepared. The ability of well-defined block copolypeptides to assemble into supramolecular copolypeptide micelles, copolypeptide vesicles, and copolypeptide hydrogels is described. Many of these assemblies have been found to possess unique properties that are derived from the amino acid building blocks and ordered conformations of the polypeptide segments.

Keywords Polypeptide, block copolypeptide, N-carboxyanhydride, living polymerization, self assembly.

Abbreviations and Symbols AM = activated monomer, ATRP = atom transfer radical polymerization, Bn-Asp = β-benzyl-L-aspartate, Bn-Glu = γ-benzyl-L-glutamate, Bn-Tyr = O-benzyl-L-tyrosine, bpy = 2,2'-bipyridine, CNS = central nervous system, depe = bis(diethylphosphino)ethane, DIC = differential interference contrast, DMEM = Dulbecco's modified eagle medium, DOPA = L-dihydroxyphenylalanine, DLS = dynamic light scattering, α-gal-C = α,D-galactopyranosyl-L-cysteine, α-gal-C^{O2} = α,D-galactopyranosyl-L-cysteine sulfone, GPC = gel permeation chromatography, HMDS = hexamethyldisilazane, LSCM = laser

scanning confocal microscopy, MALDI-MS = matrix assisted laser desorption ionization mass spectroscopy, NACE = non-aqueous capillary electrophoresis, NCA = α-amino acid N-carboxyanhydride, NGF = nerve growth factor, PA = poly(L-alanine), PBLA = poly(β-benzyl-L-aspartate), PBS = phosphate buffered saline, PBLG = poly(γ-benzyl-L-glutamate), PC = polycarbonate, PDMS = polydimethylsiloxane, PEG = polyethylene glycol, PMLG = poly(γ-methyl-L-glutamate), PMDG = poly(γ-methyl-D-glutamate), PPG = poly(*racemic*-propargylglycine), PZLL = poly(ε-carbobenzyloxy-L-lysine), ROMP = ring opening metathesis polymerization, TEM = transmission electron microscopy, TFA-Lys = ε-trifluoroacetyl-L-lysine, TMS = trimethylsilyl, Z-Lys = ε-carbobenzyloxy-L-lysine.

1 Introduction

Biological systems produce proteins that possess the ability to self-assemble into complex, yet highly ordered structures [1]. These remarkable materials are polypeptide copolymers that derive their properties from precisely controlled sequences and compositions of their constituent amino acid monomers. There has been recent interest in developing synthetic routes for preparation of these natural polymers as well as de novo designed polypeptide sequences to make products for applications in medicine (artificial tissues, implants), biomineralization (resilient, lightweight, ordered inorganic composites), and analysis (biosensors, medical diagnostics) [2].

To be successful in these applications, it is important that materials can self-assemble into precisely defined structures. Polypeptides have many advantages over conventional synthetic polymers since they are able to adopt stable ordered conformations [3]. Depending on the amino acid side chain substituents, polypeptides are able to adopt a multitude of conformationally stable regular secondary structures (helices, sheets, turns), tertiary structures (e.g. the β-strand-helix-β-strand unit found in β-barrels), and quaternary assemblies (e.g. collagen microfibrils) [3]. The synthesis of polypeptides that can assemble into non-natural structures is an attractive challenge for polymer chemists.

Synthetic peptide based polymers are not new materials: homopolymers of polypeptides have been available for many decades, yet, partially due to their heterogeneous nature, have only seen limited use as structural materials [4]. In recent decades, improved methods in chemical synthesis have made possible the preparation of increasingly complex copolypeptide sequences of controlled molecular weight that display properties far superior to ill-defined homopolypeptides [5]. Furthermore, block copolypeptides, that combine different structural and functional peptide elements, have been prepared and begin to mimic some of the complexities of proteins [6]. These polymers are well suited for applications where polymer assembly and functional domains need to be at length scales ranging from nanometers to microns. These block

copolypeptides are macroscopically homogeneous as solids, but dissimilarity between the block segments typically results in phase separation in aqueous media [7]. Synthesis of simple hydrophilic/hydrophobic diblock copolypeptides, when dispersed in water, allows formation of peptide based micelles, vesicles, and hydrogels potentially useful in biomedical applications [8]. The regular secondary structures obtainable within polypeptide segments provide opportunities for hierarchical self-assembly unobtainable with conventional block copolymers or small-molecule surfactants.

Upon examining the different methods for polypeptide synthesis, the limitations of these techniques for preparation of block copolypeptides become apparent. Conventional solid-phase peptide synthesis is neither economical nor practical for direct preparation of large polypeptides (> 100 residues) due to unavoidable deletions and truncations that result from incomplete deprotection and coupling steps. The most economical and expedient process for synthesis of long polypeptide chains is the polymerization of α-amino acid-N-carboxyanhydrides (NCAs) (Eq. 1) [9]. This method involves the simplest reagents and high molecular weight polymers can be prepared in both good yield and in large quantity with no detectable racemization at the chiral centers. The considerable variety of NCAs that have been synthesized (> 200) allows exceptional diversity in the types of polypeptides that can be prepared [9].

Insert Equation 1

Since the late 1940's, NCA polymerizations have been the most common technique used for large scale preparation of high molecular weight polypeptides [10]. However, these materials have primarily been homopolymers, random copolymers, or graft copolymers that lack the sequence specificity and monodispersity of natural proteins. The level of control in NCA polymerizations has not been able to rival that attained in other synthetic polymerizations (e.g. vinyl addition polymerizations) where sophisticated polymer architectures have been prepared (e.g. stereospecific polymers and block copolymers) [11]. Attempts to prepare block copolypeptides and hybrid block copolymers using NCAs have traditionally resulted in polymers whose compositions did not match monomer feed compositions and that contained significant

homopolymer contaminants [12]. Block copolymers could only be obtained in pure form by extensive fractionation steps, which significantly lowered the yield and efficiency of this method. The main factor limiting the potential of NCA polymerizations has been the presence of side reactions (chain termination and chain transfer) that restrict control over molecular weight, give broad molecular weight distributions, and prohibit formation of well-defined block copolymers [13]. Recent progress in elimination of these side reactions has been a major breakthrough for the polypeptide materials field. This review summarizes developments that enable the synthesis of well defined homo and block copolypeptides from controlled and living polymerizations NCA monomers. Examples of structures formed by self-assembly of block copolypeptides in solution are also described.

2 Polypeptide synthesis using NCAs

2.1 Conventional methods NCA polymerizations have been initiated using many different nucleophiles and bases, the most common being primary amines and alkoxide anions [9]. Primary amines, being more nucleophilic than basic, are good general initiators for polymerization of NCA monomers that provide relatively slow polymerization and are well understood. Tertiary amines, alkoxides, and other initiators that are more basic than nucleophilic, have found use since they are in some cases able to prepare polymers of very high molecular weight where primary amine initiators cannot. Strong base initiators generally promote much faster NCA polymerization compared to primary amine initiators, yet fine mechanistic details of these systems are poorly understood. Optimal polymerization conditions have often been determined empirically for each NCA and thus there have been no universal initiators or conditions by which to prepare high polymers from any monomer. This is in part due to the different properties of individual NCAs and their polymers (e.g. solubility) but is also strongly related to the side reactions that occur during polymerization.

Insert Equation 2

The most likely pathways of NCA polymerization are the so-called "amine" and the "activated monomer" (AM) mechanisms [9]. The amine mechanism is a nucleophilic ring

opening chain growth process where the polymer would grow linearly with monomer conversion if side reactions were absent (Eq. 2). On the other hand, the AM mechanism is initiated by deprotonation of an NCA, which then becomes the nucleophile that initiates chain growth (Eq. 3). It is important to note that a polymerization can switch back and forth between the amine and AM mechanisms many times: a propagation step for one mechanism is a side reaction for the other, and vice versa. It is because of these side reactions that block copolypeptides and hybrid block copolymers prepared from NCAs using amine initiators under conventional conditions (i.e. 20 ºC, 1 atm) have structures different than predicted by monomer feed compositions and most likely have considerable homopolymer contamination. These side reactions also prevent control of chain-end functionality desirable for many applications.

Insert Equation 3

One inherent problem in conventional NCA polymerizations is that the choice of initiator provides no control over the reactivity of the growing polymer chain-end during the course of the polymerization. Once an initiator reacts with a NCA monomer, it is no longer involved in the polymerization and the resulting primary amine, carbamate, or NCA anion endgroup is free to undergo a variety of undesired side reactions. Another problem is one of monomer purity. Although most NCAs are crystalline compounds, they typically contain minute traces of acid, acid chlorides, or isocyanates that can quench propagating chains. The presence of other adventitious impurities, such as water, can cause problems by acting as chain-transfer agents or even as catalysts for side-reactions. The high moisture, nucleophile, and base sensitivity of NCAs can make their purification challenging, especially for NCAs that are not easily crystallized. Overall, the abundance of potential side reactions present in reaction media make it difficult to achieve a living polymerization system for NCAs where only chain propagation occurs.

2.2 Initiators for transition metal catalysis A successful strategy for propagation rate enhancement and elimination side-reactions in NCA polymerizations has been the use of transition metal complexes as catalysts for addition of NCA monomers to polypeptide chain-

ends. The use of transition metals to control reactivity has been proven in organic and polymer synthesis as a means to increase reaction selectivity, efficiency, and rate [14]. Using this approach, a significant advance in the development of a general method for living NCA polymerization was realized in 1997. Highly effective zerovalent nickel and cobalt initiators (i.e. bpyNi(COD) and $(PMe_3)_4Co$) [15,16] were developed by Deming that allow the living polymerization of many different NCAs into high molecular weight polypeptides via an unprecedented activation of the NCAs to generate covalent metal containing propagating species. These propagating species were also found to be highly active for NCA addition and increased polymerization rates more than an order of magnitude compared to amine initiated polymerizations at 20 ºC. The metal ions were also found to be conveniently removed from the polymers by simple precipitation or dialysis of the samples after polymerization.

Mechanistic studies on the initiation process showed that both nickel and cobalt complexes react identically with NCA monomers to form metallacyclic complexes by oxidative addition across the anhydride bonds of NCAs [15,16]. These oxidative-addition reactions were followed by addition of a second NCA monomer to yield complexes identified as six-membered amido-alkyl metallacycles (Eq. 4). These intermediates were found to further contract to five-membered amido-amidate metallacycles upon reaction with additional NCA monomers. This ring contraction is thought to occur via migration of an amide proton to the metal-bound carbon, which liberates the chain-end from the metal (Eq. 5) [17]. The resulting amido-amidate complexes were thus proposed as the active polymerization intermediates. Propagation through the amido-amidate metallacycle was envisioned to occur by initial attack of the nucleophilic amido group on the electrophilic C_5 carbonyl of an NCA monomer (Eq. 6). This reaction results in a large metallacycle that can contract by elimination of CO_2. Proton transfer from the free amide to the tethered amidate group further contracts the ring to regenerate the amido-amidate propagating species, while in turn liberating the end of the polymer chain.

Insert Equations 4,5,6

In this manner, the metal is able to migrate along the growing polymer chain, while being held by a robust chelate at the active end. The formation of these chelating metallacyclic intermediates appears to be a general requirement for obtaining living NCA polymerizations using transition metal initiators. These cobalt and nickel complexes are able to produce polypeptides with narrow chain length distributions ($M_w/M_n < 1.20$) and controlled molecular weights ($500 < M_n < 500{,}000$) [18]. These polymerizations can be conducted in a variety of solvents (e.g. THF, DMF, EtOAc, dioxane, MeCN, DMAc, nitrobenzene) and over a broad range of temperatures (i.e. 10 to 100 ºC) with no loss of polymerization control and with dramatic increases in polymerization rate as temperature is increased. By addition of different NCA monomers, the preparation of block copolypeptides of defined sequence and composition is feasible [5,19].

This polymerization system is general, and gives controlled polymerization of a wide range of NCA monomers as pure enantiomers (D or L configuration) or as racemic mixtures. In addition to commonly used NCA monomers, such as protected lysine, glutamate, aspartate, and arginine, many hydrophobic amino acid monomers (e.g. leucine, valine, alanine, isoleucine, phenylalanine) as well as other reactive amino acids (e.g. methionine, cysteine, tyrosine, DOPA) have been successfully polymerized in a controlled manner using cobalt and nickel initiators. There is much current interest in functional and reactive polypeptides, and NCAs bearing more complex functionality have also been polymerized using this methodology. The earliest examples were controlled polymerizations of oligoethylene glycol functionalized lysines [20] and serines [21], which were later followed by polymerization of lysine based NCAs containing side-chain attached liquid crystal forming mesogens [22]. Thermoresponsive oligoethylene glycol modified glutamate NCAs have also been reported by Li to polymerize effectively using a nickel initiator [23].

Recently, the Deming lab has used cobalt initiators to polymerize sugar containing NCAs based on lysine [24] and cysteine [25], which yield fully glycosylated, high molecular weight glycopolypeptides that can adopt different chain conformations. Li and coworkers have also used

a nickel initiator to polymerize lysine based NCAs that contain side-chain activated alkyl bromide functionalities, which are useful for growth of vinyl polymers off of the polypeptide side chains using ATRP [26]. It is notable that the active metal centers do not react with the alkyl halide functionalities, which could be problematic if amine initiators were used instead. A key challenge in these recent examples was purification of the highly functional NCAs, which could not be purified by recrystallization. To solve this problem, Kramer and Deming developed an anhydrous flash column chromatography method for NCA purification that enables one to obtain a wide range of difficult to crystallize NCAs in suitable purity for controlled polymerization [27], and has made possible the preparation of many new highly functional NCAs [28].

One potential limitation of using zerovalent metal initiators is in the preparation of chain-end functionalized polypeptides, since the active propagating species are generated in situ and the C-terminal end of the polypeptide is derived from the first NCA monomer. Consequently, this method does not allow easy incorporation of functionality (e.g. polymer or small molecule) to the carboxyl chain-end. For this reason, Deming and coworkers pursued alternative methods for direct synthesis of the amido-amidate metallacycle propagating species and developed allyloxycarbonylaminoamides as universal precursors to amido-amidate nickelacycles. These simple amino acid derivatives undergo tandem oxidative-additions to nickel(0) to give active NCA polymerization initiators (Eq. 7) [29]. These complexes were found to initiate polymerization of NCAs yielding polypeptides with defined molecular weights, narrow molecular weight distributions, and with quantitative incorporation of the initiating ligand as a C-terminal end-group. This chemistry provides a facile means to incorporate diverse molecules such as polymers, peptides, oligosaccharides or other ligands onto the chain-ends of polypeptides via a robust amide linkage, and was further elaborated by Menzel's group to grow polypeptides off of polystyrene particles [30]. Recently, this methodology was used by Patton and coworkers to attach nickel initiators to silicon oxide substrates and then grow lysine-cysteine and glutamate-cysteine block copolypeptides from the surfaces [31].

Insert Equation 7

Allyloxycarbonylaminoamide precursors to NCA polymerization initiators were also recently incorporated into the side-chains of lysine based NCAs by Deming's lab [32]. These NCAs underwent controlled polymerization using a cobalt initiator to give the linear polypeptide, with no reaction of the side-chain functionality with the active propagating species or metal initiator precursors. After complete consumption of NCA monomer, and without isolation of the polypeptide, the allyloxycarbonylaminoamide side-chains were then activated by addition of stoichiometric zerovalent nickel, which generated active nickelacycle initiators in each polypeptide side-chain (Eq. 8). Addition of a second batch of NCA monomer led to growth of well-defined cylindrical copolypeptide brushes in a simple, tandem catalysis process that required no intermediate deprotection or polypeptide isolation or purification steps [32].

Insert Equation 8

In related work, Deming's lab also developed a means to functionalize the N-terminal ends of living polypeptide chains using electrophilic reagents. When a macromolecular electrophile is used, the resulting product is a polypeptide hybrid block copolymer. It is well-known in NCA polymerizations that electrophiles, such as isocyanates, act as chain terminating agents by reaction with the propagating amine chain-ends [9]. Deming and coworkers reported that the reactive living nickelacycle polypeptide chain-ends could be quantitatively capped by reaction with excess isocyanate, isothiocyanate, or acid chloride [33]. Using this chemistry, they prepared isocyanate end-capped poly(ethylene glycol), PEG, and reacted this, in excess, with living poly(γ-benzyl-L-glutamate), PBLG, to obtain PBLG-*b*-PEG diblock copolymers (Eq. 9).

Insert Equation 9

By knowing the active intermediates in these metal catalyzed polymerizations, Deming's lab was also able to use chiral donor ligands to prepare optically active nickel initiators for the enantioasymmetric polymerization of NCAs [34]. Since polypeptides are chiral polymers, the ability to control stereochemistry during polymerization is potentially important. This is especially true since the self-assembly and properties of polypeptides are critically dependent on the stereochemistry of the amino acid components. Due to constraints imposed by the initial

oxidative-addition reactions and the stability of zerovalent cobalt and nickel complexes, only a limited pool of chiral ligands could be used. For example, common chiral aryl-substituted bisphoshines were completely ineffective in promoting oxidative-additions of NCAs with nickel(0). Using optically active 2-pyridinyl oxazoline ligands that were mixed with bis(1,5-cyclooctadiene)nickel in THF, chiral nickel complexes formed that were found to selectively polymerize one enantiomer of an NCA over the other [34]. The highest selectivity was observed with the nickel complex of (S)-4-*tert*-butyl-2-pyridinyl oxazoline, which gave a ratio of enantiomer polymerization rate constants (k_D/k_L) of 5.2(0.1) (Eq. 10). This initiator also gave an 17% enantiomeric excess of the D-antipode in the copolymer formed at 16% conversion in the polymerization of racemic NCA. It was found that subtle modification of this ligand by incorporation of additional substituents had a substantial impact on initiator selectivities. These results were a first step toward the ability to readily synthesize optically pure polypeptides from inexpensive racemic monomer pools. The main limitation of this system, however, is the fluxional coordination geometry around nickel(II), which hinders the development of a rigid, chiral environment at the metal center.

Insert Equation 10

Subsequently, Deming and coworkers identified other initiating systems based on amido-sulfonamide metallacycles prepared via deprotonation of the corresponding amine complexes. Deming studied a ruthenium(II) amido-sulfonamide complex, which although not an amido-*amidate* metallacycle, was recognized to possess all the required features for controlled NCA polymerization (Eq. 11) [35]. This complex contains a nucleophilic alkyl amido group, stabilized by a rigid chelate, and a proton-accepting sulfonamide group on the other end of the metallacycle that allows the chain-end to migrate off the metal. This ruthenium complex, and the corresponding isoelectronic Cp*Iridium(III) (Cp* = C_5Me_5) complex, were found to initiate living polymerizations of NCAs [35], which shows that effective initiators can also be prepared with 2nd and 3rd row metals [36]. Furthermore, these initiators were found to give much higher enantiomeric selectivities, as well as polymerization activities, in polymerizations of racemic

NCAs compared to the nickel systems studied earlier. This work was elaborated by Lin who prepared similar amido-sulfonamide metallacycles using platinum(II), and found that these complexes give controlled polymerization of N_{ε}-carbobenzyloxy-L-lysine NCA, Z-Lys NCA (Eq. 11) [37]. Overall, it can be seen that the use of transition metal initiated NCA polymerization allows formation of well-defined copolymer architectures that rival those prepared using any polymerization system.

Insert Equation 11

2.3 Recent developments using amine initiators In the past decade, a number of new approaches have been reported to give controlled NCA polymerizations. These approaches share a common theme in that they are all improvements on the use of conventional primary amine polymerization initiators. This approach is attractive since primary amines are readily available and since the initiator does not need to be removed from the reaction after polymerization. In fact, if the polymerization proceeds without any chain breaking reactions, the amine initiator becomes the C-terminal polypeptide end-group. In this manner, there is potential to form chain-end functionalized polypeptides or even hybrid block copolymers if the amine is a macroinitiator. The challenge in this approach is to overcome the numerous side-reactions of these systems without the luxury of a large number of experimental parameters to adjust.

In 2004, the group of Hadjichristidis reported the primary amine initiated polymerization of NCAs under high vacuum conditions [38]. The strategy here was to determine if a reduced level of impurities in the reaction mixture would lead to fewer polymerization side reactions. Unlike the vinyl monomers usually polymerized under high vacuum conditions, NCAs cannot be purified by distillation. Consequently, it is unclear if NCAs can be obtained in higher purity by high vacuum recrystallization than by recrystallization under a rigorous inert atmosphere. However, the high vacuum method does allow for better purification of polymerization solvents and the *n*-hexylamine initiator. It was found that polymerizations of γ-benzyl-L-glutamate NCA, Bn-Glu NCA, and Z-Lys NCA under high vacuum in DMF solvent displayed all the characteristics of a living polymerization system [38]. Polypeptides could be prepared with

control over chain length, chain length distributions were narrow, and block copolypeptides were prepared. This method has been used by Iatrou and coworkers to prepare a number of different block copolypeptides, primarily PBLG segments connected to polymers of lysine, leucine, tryosine, as well as the imino acid proline, and their microphase separated morphologies have been studied in the bulk state [39,40].

For this method, the authors concluded that the side-reactions normally observed in amine initiated NCA polymerizations are simply a consequence of impurities. Since the main side reactions in NCA polymerizations do not involve reaction with adventitious impurities such as water, but instead reactions with monomer, solvent, or polymer (i.e. termination by reaction of the amine-end with an ester side-chain, attack of DMF by the amine-end, or chain transfer to monomer)[9], it appears removal of water or other reaction components is able to inhibit these side reactions. A likely explanation for the polymerization control observed under high vacuum is that CO_2 acts to promote side reactions of growing chains with monomer, polymer, or solvent, and its removal from the reaction medium under vacuum inhibits these reactions, and promotes controlled polymerization. A number of early and recent studies support this role of CO_2 as being detrimental to amine initiated NCA polymerizations, where for some NCAs it is able to decrease chain propagation rate by reversibly forming a carbamate with the amine end-group and may also catalyze side-reactions [41,42]. Thus, it is reasonable to speculate (*vide infra*) that removal of CO_2 from NCA polymerizations under high vacuum is the dominant factor in enabling controlled chain growth in these systems. Recently, in polymerizations of O-benzyl-L-tyrosine NCA, Bn-Tyr NCA, in DMF, it was determined that although most side reactions are insignificant in the high-vacuum polymerization, some termination of chains by reaction with DMF solvent does occur [43].

Further insights into amine initiated NCA polymerizations were also reported in 2004 by the group of Giani and coworkers [44]. This group studied the polymerization of ε-trifluoroacetyl-L-lysine NCA, TFA-Lys NCA, in DMF using *n*-hexylamine initiator at different temperatures. Contrary to the high vacuum work, the solvent and initiator were purified using

conventional methods and the polymerizations were conducted under a nitrogen atmosphere on a Schlenk line. After complete consumption of NCA monomer, the crude polymerization mixtures were analyzed by GPC and non-aqueous capillary electrophoresis (NACE). A unique feature of this work was the use of NACE to separate and quantify the amount of polymers with different chain-ends, which corresponded to living chains (amine end-groups) and "dead" chains (carboxylate and formyl end-groups from reaction with NCA anions and DMF solvent, respectively, Eq. 12 and 13). Not surprisingly, at 20 ℃, the polymer products consisted of 78 % dead chains, and only 22 % living chains, which illustrates the abundance of side reactions in these polymerizations under conventional conditions.

Insert Equations 12 and 13

An intriguing result was found for polymerizations conducted at 0 ℃ where 99 % of the chains had living amine chain ends, and only 1 % were found to be dead chains. To verify that these were truly living polymerizations, additional NCA monomer was added to these chains at 0 ℃ resulting in increased molecular weight and no increase of the amount of dead chains. While TFA-Lys NCA was the only monomer studied, this work showed that controlled NCA polymerizations can be obtained by lowering temperature. The effect of temperature is not unusual, as similar trends can be found in cationic and anionic vinyl polymerizations [45]. At elevated temperature, the side reactions have activation barriers similar to chain propagation. When the temperature is lowered, the activation barrier for chain propagation becomes lower than that of the side reactions and chain propagation dominates kinetically. A key limitation of this method is that these polymerizations are very slow at 0 ºC, often requiring numerous days to obtain polypeptide chains of modest length. A remarkable feature of this system is that increased impurity/byproduct (i.e. CO_2) levels, as compared to the high vacuum method, did not result in side reactions at low temperature. This result shows that even with CO_2 present, side-reactions in amine initiated NCA polymerzations can be made kinetically insignificant at low temperature.

Since these original studies, a number of groups have used and studied low temperature NCA polymerzations in greater detail. Shao's lab reported the synthesis of block copolypeptides

of PBLG with segments of alanine, leucine and phenylalanine at 0 ºC, and found that greater than 90% of the PBLG chains were active for the second monomer addition using MALDI-MS analysis [46]. Schouten also reported the controlled polymerization of *tert*-butyl-L-glutamate NCA at 0 ºC and use of these chains to prepare block copolypeptides with other glutamate ester NCAs [47]. Perhaps the most comprehensive studies of amine initiated NCA polymerizations at low temperature and/or under vacuum were performed by Heise and coworkers [48]. They examined ten different NCA monomers and found, using MALDI-MS analysis of end-groups, that most of these, including monomer mixtures for preparation of statistical copolymers, show fewer side-reactions at 0 ºC compared to elevated temperatures. In a follow up study, they combined low temperature polymerizatons with those run under low pressure in order to identify optimal polymerization conditions [42]. Surprisingly, only α-helical favoring monomers (Bn-Glu, alanine, Z-Lys) showed rate accelerations upon reduction in pressure (and consequent CO_2 removal), while non-helicogenic monomers (β-benzyl-L-aspartate, O-benzyl-L-serine, O-benzyl-L-threonine) were not affected by reaction pressure. Thus the use of high vacuum or other methods for CO_2 removal to obtain controlled NCA polymerization seems to be highly monomer dependent. Also the enhancements in polymerization rates seen by removing CO_2 at 20 ºC were found to be minimal at 0 ºC, thus indicating there is no advantage for conducting an NCA polymerization under reduced pressure at 0 ºC. From this study, it was concluded that helicogenic NCA monomers could be polymerized in a controlled manner at 20 ºC if CO_2 was removed from the reaction mixture, while non-helicogenic monomers should be polymerized at 0 ºC for optimal control over polymerization [42]. This strategy was validated by preparation of a tetrablock copolypeptide of PBLG-PA-PZLL-PBLA.

A different innovative approach to controlling amine initiated NCA polymerizations was reported in 2003 by Schlaad and coworkers [49]. Their strategy was to avoid formation of NCA anions, which cause significant chain termination after rearranging to isocyanocarboxylates [9], through use of primary amine hydrochloride salts as initiators. The reactivity of amine hydrochlorides with NCAs was first explored by the group of Knobler, who found that they can

react with NCAs to give single NCA addition products [50]. Use of the hydrochloride salt takes advantage of its diminished reactivity as a nucleophile compared to the parent amine, which effectively halts the reaction after a single NCA insertion by formation of an inert amine hydrochloride in the product. The reactivity of the hydrochloride presumably arises from formation of a small amount of free amine by reversible dissociation of HCl (Eq. 14). This equilibrium, which lies heavily toward the dormant amine hydrochloride species, allows for only a very short lifetime of reactive amine species. Consequently, as soon as a free amine reacts with an NCA, the resulting amine end-group on the product is immediately protonated and is prevented from further reaction. The acidic conditions also assist elimination of CO_2 from the reactive intermediate, and more importantly, suppress formation of unwanted NCA anions.

Insert Equation 14

To obtain controlled polymerization, and not just single NCA addition reactions, Schlaad's group increased the reaction temperature (40 to 80 ℃), which was known from Knobler's work to increase the equilibrium concentration of free amine, as well as increase the exchange rate between amine and amine hydrochloride [50]. Using primary amine hydrochloride end-capped polystyrene macroinitiators to polymerize Z-Lys NCA in DMF, Schlaad's group obtained polypeptide hybrid copolymers in 70 to 80% yield after 3 days at elevated temperature. Although these polymerizations are slow compared to amine initiated polymerizations, the resulting polypeptide segments were well defined with very narrow chain length distributions ($M_w/M_n < 1.03$). These distributions were much narrower than those obtained using the free amine macroinitiator, which argues for diminished side reactions in the polypeptide synthesis. The molecular weights of the resulting polypeptide segments were found to be *ca*. 20 to 30% higher than would be expected from the monomer to initiator ratios. This result was attributed to termination of some fraction of initiator species by traces of impurities in the NCA monomers, although the presence of unreacted polystyrene chains was not reported. Recently, this methodology was extended to the preparation of new hybrid copolymers of poly(Bn-Glu) from poly(2-isopropyl-2-oxazoline) [51] and PEG-amine hydrochloride [52] macroinitiators.

The use of amine hydrochloride salts as initiators for controlled NCA polymerizations shows tremendous promise. The concept of fast, reversible deactivation of a reactive species to obtain controlled polymerization is a proven concept in polymer chemistry, and this system can be compared to the persistent radical effect employed in all controlled radical polymerization strategies [53]. Like those systems, success of this method requires a carefully controlled matching of the polymer chain propagation rate constant, the amine/amine hydrochloride equilibrium constant, and the forward and reverse exchange rate constants between amine and amine hydrochloride salt. This means it is likely that reaction conditions (e.g. temperature, halide counterion, solvent) will need to be optimized to obtain controlled polymerization for each different NCA monomer, as is the case for most vinyl monomers in controlled radical polymerizations. Within these constraints, it is possible that controlled NCA homopolymerizations utilizing simple amine hydrochloride initiators can be obtained, yet this method may not be advantageous for preparation of block copolypeptides due to the need for monomer specific optimization.

Another interesting approach to obtain controlled NCA polymerization using silylated amines was reported in 2007 by Cheng. Hexamethyldisilazane (HMDS) was used to initiate polymerizations of either Z-Lys NCA or Bn-Glu NCA in DMF at ambient temperature and was found to give well-defined polypeptides of controlled chain length and low polydispersity in high yield [54]. Addition of a second batch of monomer to completed chains afforded block copolymers. Chain growth in this system does not appear to show any of the common side-reactions found in amine initiated NCA polymerization, which is attributed to the unique properties of the N-trimethylsilyl (TMS) groups. The HMDS is proposed to transfer a TMS group to the NCA followed by addition of the silylamine to the resulting intermediate (Eq. 15). This process yields a ring-opened monomer with a TMS-carbamate active end-group on the growing chain, similar to processes that occur in Group Transfer Polymerization of vinyl monomers [55]. The TMS-carbamate mediates NCA addition in a way that suppresses side-reactions. This system has an advantage in that it proceeds at much higher rates (*ca.* 12 - 24 h at

ambient temperature to obtain DP = 100) compared to low temperature or amine hydrochloride initiated polymerizations, yet still is slower than transition metal initiated systems (*ca.* 30 – 60 min at ambient temperature).

Insert Equation 15

Cheng elaborated this method by showing that a variety of TMS amines can be used as initiators in place of HMDS to give controlled polymerizations by a similar process. These initiators also provide defined C-terminal end-groups on the polypeptides from the TMS amine initiator (Eq. 16) [56]. This chain-end functionalization was found to work well for both Z-Lys NCA and Bn-Glu NCA as well as block copolymers of these monomers. The TMS-carbamate active chain-ends are highly moisture sensitive, yet this is not much of an issue since NCAs themselves are moisture senstitive and must be polymerized in an anhydrous environment. This methodology was used to prepare polypeptide-poly(norbornene diimide) brush copolymers via both “grafting from” and “grafting through” approaches [57]. In the grafting from approach, poly(norbornenes) bearing TMS amine functionalities were used as macroinitiators to grow polypeptide brush segments. In the grafting through approach, TMS amine functionalized norbornene monomers were used to prepare end-functionalized polypeptide segments that were then linked by ROMP of the norbornene end-groups.

Insert Equation 16

3 Block copolypeptide synthesis and assembly

For assembly into novel supramolecular structures, block copolypeptides are required that have structural domains (i.e. amino acid sequences) whose size and composition can be precisely adjusted. Such materials have historically proven elusive using conventional techniques. Strong base initiated NCA polymerizations are very fast. These polymerizations are poorly understood and well-defined block copolymers cannot be prepared. Primary amine initiated NCA polymerizations are also not free of side reactions. Even after fractionation of the crude preparations, the resulting polypeptides are relatively ill-defined, which may complicate unequivocal evaluation of their properties and potential applications. Nevertheless, there are

many reports on the preparation of block copolypeptides using conventional primary amine initiators [58]. Examples include many hydrophilic-hydrophobic and hydrophilic-hydrophobic-hydrophilic di- and tri-block copolypeptides (where hydrophilic residues were glutamate and lysine, and hydrophobic residues were leucine [59,60], valine [61], isoleucine [62], phenylalanine [63], and alanine [64]) prepared to study conformations of the hydrophobic domain in aqueous solution. More recently, Cameron and coworkers reported the synthesis of novel (α-helix)-*b*-(β-sheet) block copolypeptides using amine initiation [65]. These polymers were reported to have polydispersities ranging from 1.47 to 1.60.

The majority of amine initiated block copolypeptides were often subjected to only limited characterization (e.g. amino acid compositional analysis) and, as such, their structures, and the presence of homopolymer contaminants, were not conclusively determined. Some copolymers, which had been subjected to chromatography, showed polymodal molecular weight distributions containing substantial high and low molecular weight fractions [63]. The compositions of these copolymers were found to be different from the initial monomer feed compositions and varied widely for different molecular weight fractions. It appears that most, if not all, block copolypeptides prepared using amine initiators under conventional conditions have structures different than predicted by monomer feed compositions and likely have considerable homopolymer contamination due to the side reactions described above.

Block copolypeptides prepared via transition-metal mediated NCA polymerization are well-defined, with the sequence and composition of block segments controlled by order and quantity of monomer added to initiating species, respectively. These block copolypeptides can be prepared with the same level of control found in anionic and controlled radical polymerizations of vinyl monomers, which greatly expands the potential of polypeptide materials. The unique chemistry of NCAs allows these monomers to be polymerized in any order, which is a challenge in most vinyl copolymerizations, and the robust chain-ends allow the preparation of copolypeptides with many block domains (e.g. > 2). The robust nature of transition metal initiation was shown by the linear, stepwise synthesis of triblock and pentablock copolypeptides

(Eq. 17) [66]. The N-TMS amine initiators and amine initiators used under high vacuum and/or low temperature conditions have recently also been used to prepare well-defined block copolypeptides [38,55]. The self-assembly of block copolypeptides has also been under extensive investigation in recent years, typically in aqueous media to mimic biological conditions. In the following sections, the assembly of block copolypeptides into different types of supramolecular assemblies is described.

Insert Equation 17

3.1 Copolypeptide nanoparticles with hydrophobic cores Micellar nanoparticles and emulsion droplets are widely used to disperse materials for a range of food [67], cosmetic [68], and pharmaceutical [69] applications. These nanoscale assemblies are composed of amphiphilic molecules that self-assemble in water, and include the addition of an oil phase in the case of emulsions [69]. Block copolymers make up a large class of micelle forming molecules [68,70,71], and include some that contain polypeptide segments, which can be enzymatically degraded to natural metabolites and possess ordered conformations not found in conventional polymers. Numerous "rod-coil" micelles have been prepared using α-helical hydrophobic polypeptides conjugated to hydrophilic polyethylene glycol (PEG) segments, such as PEG-b-PBLG [72,73] and PEG-b-PBLA [74]. β-strand polypeptide segments have also been used to facilitate interchain interactions and increase micelle stability [75]. On the contrary, micelles prepared solely from polypeptide segments have not been reported until recently. One key reason is the structure inherent in peptides which typically favors extended conformations and strong interchain interactions, which usually prevent formation of a disordered spherical micelle core.

The Deming lab was able to prepare block copolypeptide micelles by incorporating disordered racemic hydrophobic segments, which allow packing of the chains into spherical micelles (Figure 1). They synthesized nonionic, block copolypeptides, poly(N_ε-2-[2-(2-methoxyethoxy)ethoxy]acetyl-L-lysine)-*block*-poly(*racemic*-leucine), or $K^P_x(rac\text{-}L)_y$, where *x* and *y* are the number of residues in each segment, which have a "reversed" rod-coil structure composed of a hydrophilic, rod-like, α-helical segment attached to a disordered, racemic

hydrophobic segment. The self assembly of these block copolypeptides in water was studied, and their compositions were optimized to identify a sample, $K^{P}_{100}(rac\text{-}L)_{10}$, which was able to form well defined micelles that are very stable against dilution, high temperatures, and various media [76]. Micelle structure was determined using a combination of transmission electron microscopy (TEM) and dynamic light scattering (DLS) measurements, where they observed formation of well-defined, stable spherical copolypeptide micelles approximately 80 nm in diameter (Fig. 1). Furthermore, they were able to encapsulate the anticancer drug camptothecin into the micelles with an efficiency of 76%, showing the potential of these carriers for drug delivery applications.

Insert Figure 1

In a related project, the Deming lab had also investigated the use of diblock copolypeptides containing racemic hydrophobic segments as surfactants for stabilization of nanoemulsion droplets [77]. In these studies, the racemic hydrophobic segment provides better miscibility with the oil phase compared to enantiomerically pure hydrophobic polypeptide segments, and give much higher surface activity. The resulting emulsions were very stable, and were obtained with nanoscale (10 to 100 nm) diameters using microfluidic homogenization, making them attractive for delivery of hydrophobic cargos. Remarkably, it was found that the copolypeptide amphiphiles also promote formation of very stable double emulsion droplets that for the first time could be prepared with outer droplet diameters down to 10 nm [77]. The block copolypeptide surfactants they designed have the general structure poly(L-lysine·HBr)$_x$-*b*-poly(racemic-leucine)$_y$, $K_x(rac\text{-}L)_y$, where x ranged from 20 to 100, and y ranged from 5 to 30 residues. Diblock copolypeptides were screened for emulsification activity by adding silicone oil (PDMS) to aqueous $K_x(rac\text{-}L)_y$ solutions followed by rotary homogenization and then high-pressure microfluidic homogenization. All $K_x(rac\text{-}L)_y$ samples gave stable nanoemulsions that did not ripen or phase separate for over 9 months. In addition to PDMS, other immiscible liquids such as dodecane, soybean oil, and methyl oleate gave emulsions using 1 mM $K_{40}(rac\text{-}L)_{20}$ in water. The versatility of this system was shown by formation of stable double emulsions using

R_{40}(*rac*-L)$_{10}$ or E_{40}(*rac*-L)$_{10}$, containing guanidinium or carboxylate functionality of L-arginine (R) and L-glutamate (E), respectively [77].

To demonstrate their encapsulating ability, both water-soluble and oil soluble fluorescent markers were loaded into copolypeptide stabilized double emulsions. Water-soluble InGaP/ZnS quantum dots were mixed with fluorescein labeled K_{40}(*rac*-L)$_{10}$ prior to emulsification with silicone oil containing pyrene. Using fluorescence microscopy, both markers and the labeled polypeptide were imaged in the double emulsion droplets (Fig. 2) [77]. Recently, the Deming lab attached the ligand biotin to the polypeptide surfactants (i.e. biotin-K_{55}(*rac*-L)$_{20}$) and used these to form stable nanoemulsions capable of specific binding to avidin proteins, such as NeutrAvidin [78]. This specific complexation allows preparation of well-defined, nanoscale droplets that present a surface coated with NeutrAvidin proteins. They showed that these materials can then be specifically coated with biotinylated ligands, such as polymers or bioactive molecules like antibodies or ligands for cell receptors. These conjugates show promise for targeted drug delivery as well as presentation of bioactive ligands or immunostimulating molecules in vaccines.

Insert Figure 2

Another type of block copolypeptide nanocarrier was developed using a unimolecular star architecture and was reported by Liu and coworkers [79]. They reacted terminal amine groups on a small polyethyleneimine core successively with a hydrophobic NCA (leucine or phenylalanine) followed by Bn-Glu NCA to yield star polymers with hydrophilic coronas and hydrophobic cores. These materials were found to be able to encapsulate hydrophobic or cationic probe molecules, where the cationic probes were bound as counterions to the anionic polyglutamate segments. In summary, although nanoparticles composed solely of polypeptide components are relatively recent developments, there is substantial interest in this area and it is likely that a wide variety of new materials and structures will be forthcoming.

3.2 Copolypeptide vesicles Membranes are important materials for many applications, ranging from separations, to devices such as sensors and fuel cells, to encapsulation of sensitive

materials, and to biomedical applications such as drug delivery. Vesicles constructed from polymers offer many advantages and opportunities over lipid vesicles for all of these applications (e.g. increased stability, tunable functionality and permeability) [80]. To date, many types of block copolypeptide amphiphiles that form stable vesicular assemblies have been developed. The first of these utilized diethylene glycol modified lysine residues, i.e. K^P, that impart both non-ionic water solubility as well as ordered α-helical conformations to the hydrophilic polypeptide domains [81]. A majority of other materials utilize highly charged polyelectrolyte segments to impart both functionality and fluidity to the membranes. More recently, these copolypeptides have included increasingly complex functionality to assist in cargo loading, vesicle targeting, and vesicle disruption.

In 2004, Deming's lab studied the roles of chain length and block composition on the assembly of uncharged diblock copolypeptide amphiphiles of the general structure: poly(N_ε-2-[2-(2-methoxyethoxy)ethoxy]acetyl-L-lysine)-*block*-poly(L-leucine), or $K^P_xL_y$ [81]. These diblock copolypeptide amphiphiles associate very strongly and essentially do not exist as single chains in aqueous solution. This property, in most cases, results primarily in the formation of irregular aggregates if the polymers are simply dispersed in deionized water. A protocol was developed, using organic solvent (THF) and a denaturant (TFA) that allowed annealing of these materials when water is added. Dialysis of the samples allows one to obtain regular assemblies in pure water.

Using this procedure, a number of amphiphilic copolymers were studied where the hydrophilic domains were varied from 60 to 200 residues in average length; and the hydrophobic domains were varied from 10 to 75 residues in average length [81]. All block copolypeptides were expected to adopt rod-like conformations due to the strong α-helix forming tendencies of both the leucine and ethylene glycol-modified lysine residues [20]. These rod-like conformations provided a flat amphiphile interface upon association in water, thus directly tying polymer conformation to supramolecular structure. Circular dichroism spectroscopy of the copolymers in water confirmed that all samples were α-helical. Using differential interference contrast (DIC)

optical microscopy, TEM, laser scanning confocal microscopy (LSCM), and DLS as initial methods to study the assemblies, some trends were identified [81]. When the hydrophobic poly(leucine) domains were less than 20 residues in length, a significant fraction of oblong or irregular micelles (ca. 100 nm diameter) were observed to form by DLS and TEM. When the size of the hydrophilic domain was 100 residues, unilamellar vesicles were observed to form with a size range of approximately 2 μm to 15 μm diameter (Fig. 3). When the hydrophilic block was increased to 150 residues, the vesicles were much larger in size, approaching 50 μm in diameter. Finally, when the hydrophilic segments were increased to 200 residues long, membrane curvature was hindered such that the major structures formed were flat membrane sheets.

Insert Figure 3

These block copolypeptides, where both hydrophilic and hydrophobic segments were α-helical, gave rise to very stiff membranes, as suggested by the large vesicle diameters and lack of fluidity in the sheets that were formed. Further investigation revealed that these membranes were completely insensitive to osmotic stress, a consequence of their impermeability to water, ions or other small molecules [81]. They also could not be reduced in size by liposome-type extrusion techniques, and could only be made smaller by more aggressive sonication methods. The inability of the uncharged vesicles to pass through small pore diameter filters was likely due to membrane rigidity and virtual absence of chain flexibility. One advantage of these materials for many applications is the media insensitivity of the ethylene glycol coating on the membrane surface. These vesicles were inert toward different ionic media, variations in pH, and the presence of large macromolecules, such as proteins in serum. However, the rigidity of these chains created drawbacks in sample processing, namely the need to use denaturants for vesicle formation, which may be problematic for encapsulation of sensitive materials, and difficulty in preparing nanoscale vesicles due to high membrane rigidity.

In 2005, Lecommandoux's group reported on the self assembly behavior of a short, zwitterionic diblock copolypeptide, poly(L-glutamatic acid)-*b*-poly(L-lysine), $E_{15}K_{15}$ [82]. This

polymer has the interesting characteristic that in aqueous solutions near neutral pH (5 < pH < 9), both segments are charged and the polypeptide is dispersed as soluble chains. However, if pH is lowered to values below ph = 4 or raised above pH = 10, one of the segments is neutralized and the chains self assemble into small vesicles. By adjustment of pH, vesicles with either anionic (high pH) or cationic (low pH) surfaces could be prepared, hence their description as "schizophrenic" vesicles. It is notable that these chains are soluble in water when both segments are highly charged, considering that the formation of water insoluble polyion complexes between poly(L-lysine) and poly(L-glutamatic acid) is well documented [83]. A key feature of this work is the utilization of short polyelectrolyte segments, which limits such polyion complex formation in dilute solutions.

Deming's group also reported in 2005 on the assembly of charged diblock copolypeptide amphiphiles, utilizing the structure directing properties of rod-like α-helical segments only in the hydrophobic domains. Specifically, the aqueous self-assembly of a series of poly(L-lysine)-*b*-poly(L-leucine) block copolypeptides was studied: K_xL_y, where *x* ranged from 20 to 80, and *y* ranged from 10 to 30 residues, as well as the poly(L-glutamatic acid)-*b*-poly(L-leucine) block copolypeptide, $E_{60}L_{20}$ [84]. In other work, it was found that samples with high K to L molar ratios (e.g. $K_{180}L_{20}$) could be dissolved directly into deionized water, yielding transparent hydrogels composed of twisted fibrils (*vide infra*) [85]. It was reasoned that use of shortened charged segments would relax repulsive polyelectrolyte interactions and allow formation of charged polypeptide membranes. Samples were processed by suspending the polymers in THF/water (1:1) followed by dialysis. Analysis of these assemblies using DIC optical microscopy revealed the presence of large, sheet-like membranes for $K_{20}L_{20}$, and thin fibrils for $K_{40}L_{20}$. The $K_{60}L_{20}$ sample was most promising, as only large vesicular assemblies were observed by DIC [84].

The $K_{60}L_{20}$ polypeptide vesicles obtained directly from dialysis are polydisperse and range in diameter from *ca*. 5 μm down to 0.8 μm as determined using DIC and DLS (Fig. 4). For applications such as drug delivery via blood circulation, a vesicle diameter of *ca*. 50 to 100 nm is

desired. It was observed that aqueous suspensions of $K_{60}L_{20}$ vesicles could be extruded through nuclear track-etched polycarbonate (PC) membranes with little loss of polypeptide material. After two passes through a filter, reductions in vesicle diameter to values in close agreement to filter pore size were observed. These results showed that the charged copolypeptide vesicles are readily extruded, allowing good control over vesicle diameter in the tens to hundreds of nanometers range (Fig. 4). DLS analysis revealed that the extruded vesicles were also less polydisperse than before extrusion and contained no micellar contaminants. The vesicular morphology was also confirmed through TEM imaging of the sub-micron $K_{60}L_{20}$ suspensions. Thus, it appears that the membranes of the $K_{60}L_{20}$ vesicles are more flexible and compliant than those of purely rod-like uncharged polypeptides. The extruded vesicles were monitored for 6 weeks using DLS and were found to be stable. The vesicles were also found to have high thermal stability. An aqueous suspension of 1 μm vesicles was held at 80 ℃ for 30 minutes, after which no vesicle disruption could be detected [84]. Only after heating to 100 ℃ for 30 minutes were the vesicles disrupted, yielding large flat membrane sheets.

Insert Figure 4

Stability of these highly charged polypeptide vesicles in ionic media is important for use in most applications ranging from personal care products to drug delivery. Although the $K_{60}L_{20}$ vesicles are unstable at high salt concentrations (>1 M), they are stable in 100 mM PBS buffer as well as serum-free DMEM cell culture media [84]. Addition of serum, which contains anionic proteins, resulted in vesicle disruption, most likely due to polyion complexation between the serum proteins and the oppositely charged polylysine chains. Accordingly, it was observed that the negatively charged polypeptide vesicles prepared using $E_{60}L_{20}$ are stable in DMEM with 10% fetal bovine serum. Based on these results, these charged polypeptide vesicles may have potential as encapsulants for water soluble therapeutics as an alternative to liposomes. These copolypeptides retain much of the stability of the uncharged polypeptide vesicles described earlier, but allow straightforward encapsulation and size control due to much simpler processing [84]. Another feature of these charged polypeptide vesicles is the potential for facile

functionalization of the hydrophilic polypeptide chains at the vesicle surface through either chemical conjugation to amine or carboxylate residues [86], or by careful choice of charged residues.

Addressing this point, Deming's lab reported the preparation of arginine-leucine (i.e. $R_{60}L_{20}$) vesicles that are able to readily enter cells due to the many guanidinium groups of the arginine segments [87]. In this case, the arginine residues played a dual role, where they were both structure directing in vesicle formation, as well as functional for cell binding and entry. Studies on endocytotsis and intracellular trafficking of these vesicles revealed that they enter HeLa cells primarily via macropinocytosis [88]. They were found to then primarily reside in early endosomes, but not in lysosomes, and although some manage to escape into cytoplasm many are trapped within these compartments. Regardless, another study showed that $R_{60}L_{20}$ vesicles were effective at condensing plasmid DNA and transfecting it into a variety of cell lines, showing the vesicles do have potential for intracellular delivery [89]. These DNA carriers are advantageous over many other transfection agents due to their low cytotoxicity.

From the pioneering studies on block copolypeptide vesicles described above, design criteria were established for successful vesicle formation, namely an α-helical hydrophobic domain connected to a charged hydrophilic domain. Since this original work, many labs have prepared different variants of block copolypeptide vesicles based on this scheme. In 2007, Hadjichristidis reported lysine-PBLG-lysine (i.e. $K_xPBLG_yK_x$) triblock copolypeptides, where the helical PBLG core favors vesicle formation [90]. Jing and coworkers prepared vesicle forming lysine-phenylalanine (K_xF_y) copolypeptides, containing α-helical phenylalanine segments [91]. These vesicles were also found to be useful in encapsulating hemoglobin and acting as oxygen carriers. Deming's lab also reported the formation of vesicles from dual hydrophilic triblock copolypeptides composed of arginine-glutamate-leucine ($R_xE_yL_z$) or pegylated lysine-arginine-leucine ($K^P{}_xR_yL_z$) sequences [92]. The use of triblock architectures was intended to retain some homoarginine residues for cell uptake, but have the majority of the hydrophilic segments be anionic or uncharged to minimize cytotoxicity, all without disrupting

vesicle formation. A number of different compositions were prepared and it was found that, although vesicles exhibiting low cytotoxicity could be formed with a $R_5E_{80}L_{20}$ copolypeptide, the R segments were unable to promote intracellular uptake. With the $K^P_xR_yL_z$ samples, the presence of the "pegylated" outer blocks was able to diminish cytotoxicity while still allowing the center R segments to promote cellular uptake [92].

Using a different approach toward vesicle formation, Jan and coworkers prepared lysine-glycine (i.e. K_xG_y) copolypeptides, where the polyglycine segment does not adopt an α-helical conformation, and has inherent higher flexibility compared to helical segments [93]. Due to the lack of a rigid hydrophobic segment, and due to the hydrophilicity of glycine compared to leucine or phenylalanine, much longer "hydrophobic" segments were needed to drive self-assembly in water and vesicle formation. A $K_{200}G_{50}$ block copolypeptide was found to form vesicles in water using MeOH/H_2O processing, and was also mineralized with silica for entrapment of molecules [94].

Other recent variants of block copolypeptide vesicles have incorporated functionality within one of the segments. In 2010, Deming's lab reported the preparation of lysine-dihydroxyphenylalanine (i.e. $K_{60}DOPA_{20}$) based vesicles, where the hydrophobic DOPA segments have the added feature of being sensitive toward oxidation [95]. DOPA residues are found naturally in mussel byssus and are important components in the ability of byssal threads to adhere underwater and to crosslink into rigid networks [96]. In a biomimetic process $K_{60}DOPA_{20}$ vesicles were oxidized in aqueous media resulting in crosslinking of the vesicle membranes (Eq. 18). The resulting membranes were very robust, and stable to organic solvents, freeze drying and osmotic shock. Similar materials, in the form of glutamate-lysine/DOPA (i.e. $E_x(K_m/DOPA_n)_y$) copolymers were reported in 2012 by Qiao [97], where the hydrophobic domains were statistical copolymers of different ratios (m:n) of lysine and DOPA that could be assembled and oxidized to crosslinked vesicles at high pH.

Insert Equation 18

There is much current interest in synthesis of glycosylated polypeptides, and vesicle forming amphiphilic copolypeptides that contain sugars in the hydrophilic corona have now also been prepared. In 2012, Lecommandoux and Heise reported the preparation of Bn-Glu-propargyl glycine (i.e. $PBLG_{20}PPG_{25}$) diblock copolymers [98]. The propargyl side-chains were then modified by copper catalyzed azide-alkyne cycloaddition with azide-functionalized galactose to give the amphiphilic glycopolypeptide (Eq. 19). Since the PPG segment is racemic, it adopts a disordered conformation in glycosylated form. The resulting rod-coil amphiphile was found after DMSO-water processing to assemble into vesicles that were able to bind their complimentary lectin. Deming's lab, in 2013, reported a different system prepared from a galactosylated NCA, α,D-galactopyranosyl-L-cysteine (α-gal-C) NCA and leucine of the composition $(\alpha\text{-gal-C})_{65}L_{20}$, which was able to form vesicles when the side-chain thioether functionalities were oxidized to sulfone groups and after THF-water processing (Fig. 5) [99]. The parent polymer, while water soluble, is α-helical, which prohibits formation of small spherical vesicles. The fully oxidized sulfone derivative, i.e. $(\alpha\text{-gal-C}^{O2})_{65}L_{20}$, is more polar, increasing its water solubility, and more importantly has a disordered conformation which assists in vesicle membrane formation. In summary, the formation of vesicles has been one of the major applications of block copolypeptides. Early work developed guidelines for formation of these structures, while current work is aimed at increasing the potent functionality and biologically interactive properties of these materials.

Insert Equation 19

Insert Figure 5

3.3 Copolypeptide hydrogels Hydrogels are a class of materials that have significant promise for use in soft tissue and bone engineering, as well as localized drug delivery [100]. The key feature of hydrogels that makes them attractive for these applications is their well hydrated, porous structure that can mimic natural extracellular matrices [101]. To replace natural materials, however, many structural and functional features must be built into synthetic hydrogels. Desirable features include: biocompatibility; degradability to allow cell in growth;

injectability and fast setting in the wound site; mechanical properties that can be tuned for different uses; control over cell adhesion to the hydrogel matrix; and tunable sustained release of growth factors and biologically active agents [102]. There are many examples where some, or even most of these features have been incorporated into hydrogels [103]. However, in many cases, hydrogel synthesis and formation becomes very complicated, which limits the practicality of such materials. More importantly, the complexity of these systems, combined with limited means for adjustment of molecular parameters, leads to the inability for independent adjustment of most of the features. For example, it would be advantageous to be able to adjust scaffold rigidity while maintaining a constant hydrogel mesh size. Such a system would allow one to directly measure the effects of scaffold rigidity on cell proliferation. Also, since hydrogel degradation is commonly accomplished using degradable crosslinkers (e.g. in PEG based hydrogels) [102], it can be difficult to adjust degradation rate without also altering crosslink density, and hence initial gel mechanical properties [102]. It would be advantageous to have a hydrogel system where many of these desired adjustable features (e.g. gel strength, gel density, adhesive capability, degradation rate, growth factor release rate) could be controlled more or less independently so that meaningful evaluations of their roles in applications could be systematically evaluated. Currently, in many systems it is difficult to identify the most important gel characteristics, since many features are adjusted simultaneously [103]. Synthetic block copolypeptide hydrogels provide a platform that allows fine adjustment of many of these parameters as well as incorporation of the essential features required for tissue engineering and drug delivery applications.

The Deming lab has developed hydrogels based on amphiphilic block copolypeptides possessing many features that make them attractive as candidates for medical applications [85]. Foremost, through combination of chemical synthesis and structural characterization a detailed understanding of structure-property relationships in these materials has been established, allowing a high level of control over gel strength, gel porosity, gel functionality, and media stability; many which can be adjusted independent of each other [19]. Second, these physically

associated gels are readily injectable through a 30G needle for facile application and filling of wound cavities [85]. Finally, the hydrogels can be prepared to be minimally toxic to cells in culture [104]. Hydrogel formation was first discovered in a series of diblock copolypeptides containing a charged, water solubilizing domain (poly(L-lysine·HBr), K; or poly(L-glutamate Na salt), E) and a α-helical hydrophobic domain (poly(L-leucine), L), i.e. K_xL_y or E_xL_y (Fig. 6) [85]. Hydrogel formation is the result of self-assembly of these polymeric amphiphiles by direct dissolution in water, and the resultant gels possess a network structure composed of nanoscale to microscale porosity and significant material rigidity despite being composed of > 95% water. In order to determine the role played by each copolypeptide domain, a comprehensive study was performed using an array of samples where both overall chain segment lengths and hydrophilic to hydrophobic compositions were systematically varied. It was found that chain length modification of both positively charged polyelectrolyte and hydrophobic segments had significant effects on properties [85]. It is worth noting that analogous samples prepared with negatively charged polyelectrolyte domains, i.e. poly(L-glutamate), were found to behave similarly, which opens the possibility of preparation of both cationic and anionic hydrogels.

Insert Figure 6

Compositional studies with different copolypeptides revealed many trends relating molecular parameters to hydrogel properties. First, as oligoleucine composition was increased gel strength was found to increase dramatically. Furthermore, only hydrophobic segments with α-helical conformations were found to form strong gels, as evidenced by the inability of a $K_{160}(\textit{rac}\text{-L})_{40}$ sample, where the racemic residues yield a disordered conformation, to form strong hydrogels. It was found that longer polyelectrolyte segments increase interchain repulsions such that the packing of the hydrophobic helices, which prefer formation of flat 2D sheets [81], must distort to minimize the overall energy of the system. The most efficient way to do this, while maintaining favorable helix packing, is to twist the sheets into fibrillar tapes, where tape width is determined by the degree of twist [105]. In this model, the helices are still able to pack perpendicular to the fibril axis, but with a slight twist between planes of parallel packed helices

(Fig. 6). TEM imaging of the nanostructure in $K_{180}L_{30}$ does, in fact, reveal a more fibrillar, tape-like nanostructure constituting the hydrogel network (Fig. 6). Overall, copolypeptide gel strength can be adjusted by many molecular parameters: overall chain length, hydrophilic to hydrophobic composition, and block architecture, in addition to the conventional method of varying copolymer concentration. By having many means to adjust gel strength, it is possible to optimize or adjust other hydrogel properties (i.e. mesh size, injectability, or surface functionality) while keeping gel strength constant.

To test their suitability for cell culture applications, hydrogel samples were also prepared in DMEM and DMEM with 5% fetal calf serum and penicillin [106]. Samples of $K_{170}L_{30}$ hydrogels were found to be stable and remained transparent in these media, which was somewhat surprising, since they contain numerous multivalent ions and anionically charged proteins. It is likely that the proteins coat the polylysine segments in the gel since it is known that polylysine homopolymer will complex with many serum proteins in solution [107]. Apparently, the resulting polyelectrolyte complexes retain enough charge or hydrophilicity to solubilize the hydrophobic gel scaffold and prevent precipitation and collapse of the network. The porous microscale morphology was found to persist in the $K_{170}L_{30}$ hydrogels in both the presence of 150 mM NaCl and in DMEM cell culturing medium. Also, cryogenic TEM revealed that the porous nanostructure persists in the presence of salt as well. The presence of the porosity and the robustness of the nanostructure even in the presence of significant ionic concentration is a critical self-assembling material characteristic for medical applications. Overall, these copolypeptide hydrogels display remarkable stability in the presence of ionic species. Hydrogels formed from helical or β-sheet-forming proteins and peptides typically show some sensitivity to ions, either requiring them to form gels, or disrupting in their presence [108,109]. Likewise, hydrogels prepared from synthetic polyelectrolytes (e.g. crosslinked polyacrylic acid) are very sensitive to salts, shrinking dramatically as ionic strength is increased [110]. The gelation mechanism for these polypeptides, the association of hydrophobic helices, provides a robust structure that is

unperturbed under a variety of conditions, including variation of pH, ionic strength, and temperature.

In effort to further understanding on hydrogel formation and tuning of mechanical properties, Deming's lab investigated $K_xL_yK_z$ triblock architectures, which were found to allow for additional tuning of hydrogel properties (Fig. 7) [66]. In particular, triblocks gave higher gel moduli and improved stability to ionic media compared to diblock copolymers of identical composition. These changes were found to be due to the increased density of K chains at the amphiphile interface, since each hydrophobic segment has a polylysine at both ends compared to only one end for the diblock samples, where this additional steric bulk acts to enhance copolymer assembly into the fibrillar morphology that gives strong networks. Deming's lab later studied pentablock copolypeptides of the structure $K_xL_yK_zL_yK_x$ that were expected to possess attributes similar to $K_xL_yK_z$ triblock copolymers, since both have associating L segments capped on each side by K segments (Fig. 7) [66]. Due to the presence of two α-helical L segments per chain, the pentablocks also have the intriguing potential for organized intrachain folding, akin to natural proteins, in addition to intermolecular assembly.

Insert Figure 7

Pentablock copolypeptides of the composition $K_{60}L_{20}K_zL_{20}K_{60}$, where *z* was varied from 10 to 200, were synthesized by stepwise linear block copolymerization using $(PMe_3)_4Co$ initiator in THF, followed by removal of protecting groups and purification. Deming's lab found that $K_{60}L_{20}K_{10}L_{20}K_{60}$ formed clusters of micelle-like aggregates with diameters ranging from 50 to 200 nm, which differed greatly from the fibrillar structures seen with diblock and triblock samples. On the other hand, the $K_{60}L_{20}K_xL_{20}K_{60}$ copolypeptides, when $z > 60$, self-assembled in water to form fibrillar hydrogel assemblies. Furthermore, adjustment of the central K segment length allowed tuning of assembly morphology and hydrogel properties where it was observed that G′ increased and minimum gelation concentration decreased as the pentablock central K segments were lengthened. The ability to control intramolecular versus intermolecular assembly of the two hydrophobic L segments in these pentablock sequences gave substantial enhancement

of hydrogel properties compared to the corresponding diblock and triblock architectures [66]. The ability to tune intrachain interactions in these materials via molecular design also is a key advance in biomimetic assembly.

Inorganic-organic biocompatible composites have tremendous potential for therapeutic and diagnostic materials applications. Block copolypeptide hydrogels are promising templates for formation of porous composites, where the porous gel scaffold can serve as a template for mineral growth. In 2009, Mallapragada and coworkers reported use of $K_{170}L_{30}$ hydrogels as templates for assembly of calcium phosphate nanocomposites [111]. The porous nature of the hydrogels, and their ability to form gels at low concentrations, allowed composites to be formed that contained up to 50% inorganic material, approaching the inorganic content of bone. Furthermore, detailed characterization of the composites revealed the mineral phase to be carbonated hydroxyapatite, with elongated platelike morphology of nanoscale dimensions, similar to natural bone. In a similar study, Li's group studied the ability of a series of K_xL_y hydrogels ($170 < x < 440$; $10 < y < 30$) to direct silica morphology by sol-gel condensation of tetramethylorthosilicate in the presence of the hydrogels [112]. They found that both the polypeptide lengths, as well as nature of anionic counterions used, had significant effects on resulting silica morphology, where either plates or rods of silica could be formed.

Initial quantitative measurements of polypeptide cytotoxicity involved cell culture within three dimensional hydrogel substrates in cell culturing medium [104]. Although polylysine is known to be cytotoxic at when free in solution [113], use of higher concentrations of polypeptide above gelation concentrations revealed that both cationic and anionic functionalized gels were promising substrates for short-term cell culture. It is likely that the hydrogel network prevents bulk diffusion of gel-bound lysine chains limiting the amount of polylysine that can interact with the cells. Although the cells remained viable, in neither gel was cell attachment or proliferation observed. The cells, in the presence of either hydrogel matrix, retain their spherical shape after 4 and up to 24 hours. Although it appears cell binding epitopes need to be incorporated into these hydrogels, their peptidic backbone provides many advantages for use of these materials as

scaffolds. These include the straightforward incorporation of chemical functionality by use of functional amino acids, as well as enzymatic degradability.

Following up on this work, Sofroniew and Deming studied the biocompatibility of diblock copolypeptide hydrogels in vivo in mouse central nervous system (CNS) tissue [114]. This work was undertaken since biomaterials represent a major opportunity for developing novel CNS treatment strategies based on site-specific delivery of scaffolds that promote the growth and migration of axons or cells derived from host or grafts, or as depots that release diffusible bioactive molecules to act in a locally restricted manner inside the blood brain barrier. A range of diblock copolypeptide hydrogel formulations with rheological properties similar to brain tissue were injected into mouse forebrain and examined after 1–8 weeks using light microscopy, immunohistochemistry and electron microscopy. Hydrogel deposits were found to elicit no more gliosis, inflammation, or toxicity to neurons, myelin or axons than did injections of physiological saline. The size, rigidity, and density of the hydrogel deposits could be varied subtly by altering sample composition and concentration. The $K_{180}L_{20}$ hydrogel was selected for detailed analyses because it formed deposits with desirable physical properties and since lysine is routinely used as a substrate for neural cell cultures. Deposits of unmodified $K_{180}L_{20}$ exhibited time-dependent in-growth of blood vessels and of certain glial cells, and limited in-growth of nerve fibers (Fig. 8). These findings showed that block copolypeptide hydrogels are injectable, re-assemble in vivo to form three dimensional deposits, exhibit little or no detectable toxicity in the CNS, integrate well with brain tissue and represent a new class of synthetic biomaterials with potential for applications as depots or scaffolds in the CNS [114].

Insert Figure 8

In a follow up study, Sofroniew and Deming examined the loading and release of bioactive hydrophilic molecules from $K_{180}L_{20}$ and $E_{180}L_{20}$ hydrogels in vitro and in vivo [115]. In vitro tests demonstrated sustained release from dialysis cassettes of the representative protein, lysozyme, dissolved in $K_{180}L_{20}$ or $E_{180}L_{20}$ hydrogels. Release times of molecules in vitro varied in relation to DCH charge and mechanical properties, and ionic strength of the media. To evaluate

bioactive protein delivery in vivo, they used nerve growth factor (NGF) and measured the size of mouse forebrain cholinergic neurons, which respond to NGF with cellular hypertrophy (Fig. 9). In comparison with NGF injected in buffer, depots of NGF dissolved in either $K_{180}L_{20}$ or $E_{180}L_{20}$ provided significantly longer delivery of NGF bioactivity, maintaining hypertrophy of local forebrain cholinergic neurons for at least 4 weeks and inducing hypertrophy a further distance away (up to 5 mm) from injection sites [115]. These findings show that depots of block copolypeptide hydrogels injected into CNS can provide sustained delivery within the blood brain barrier of a bioactive protein growth factor that exerts a predicted, quantifiable effect on local cells over a prolonged subacute time.

Insert Figure 9

4 Conclusions

The synthesis of polypeptides by ring opening polymerization is an area that has been under study for more than five decades. Initially, this field suffered from limitations that necessitated excessive sample purification and fractionation to obtain well-defined polypeptides. Over the last 15 years, vast improvements in NCA polymerizations now allow the synthesis of a variety of block copolypeptides of controlled dimensions (molecular weight, sequence, composition, and molecular weight distribution). Many different block copolypeptides have now been prepared, and used to form self-assembled structures with promising properties. The ability to easily adjust chain conformation and functionality in polypeptides, in combination with advanced synthetic methods that enable preparation of complex sequences, has opened up a new, promising field of materials with a wide range of tunable properties.

References

1) Branden C, Tooze J (1991) Introduction to Protein Structure, Garland, New York

2) (a) Cha JN , Stucky GD, Morse DE, Deming TJ (2000) Nature 403:289 (b) van Hest JCM, Tirrell DA (2001) Chem. Commun. 1897

3) Voet D, Voet JG (1995) Biochemistry 2nd edn. Wiley, NY, chap 32

4) (a) Fasman GD (1967) Poly α-Amino Acids, Dekker, New York (b) Fasman GD (1989) Prediction of Protein Structure and the Principles of Protein Conformation, Plenum Press, New York, p 48

5) Deming TJ (2000) J. Polym. Sci. Polym. Chem. Ed. 38:3011

6) Deming TJ (2012) Top. Curr. Chem. 310:1

7) Discher DE, Eisenberg A (2002) Science 297:967

8) Kwon GS, Naito M, Kataoka K, Yokoyama M, Sakurai Y, Okano T (1994) Colloids and Surfaces B: Biointerfaces 2:429

9) (a) Kricheldorf HR (1987) α-Aminoacid-N-Carboxyanhydrides and Related Materials, Springer-Verlag, New York (b) Kricheldorf HR (1990) In: Penczek S (ed) Models of Biopolymers by Ring-Opening Polymerization, CRC Press, Boca Raton

10) Woodward RB, Schramm CH (1947) J. Am. Chem Soc. 69:1551

11) Webster O (1991) Science 251:887

12) (a) Cardinaux F, Howard JC, Taylor GT, Scheraga HA (1977) Biopolymers 16:2005 (b) Howard JC, Cardinaux F; Scheraga HA (1977) Biopolymers 16:2029 (c) Kubota S, Fasman GD (1975) Biopolymers 14:605

13) (a) Sekiguchi H (1981) Pure and Appl. Chem. 53:1689 (b) Sekiguchi H, Froyer G (1975) J. Poly. Sci. Symp. 52:157

14) Collman JP, Hegedus LS, Norton JR, Finke RG (1987) Principles and Applications of Organotransition Metal Chemistry 2nd edn, University Science, Mill Valley

15) (a) Deming TJ (1997) Nature 390:386 (b) Deming TJ (1998) J. Am. Chem. Soc. 120:4240

16) Deming TJ (1999) Macromolecules 32:4500

17) Deming TJ, Curtin SA (2000) J. Am. Chem. Soc. 122:5710

18) Deming TJ (2002) Adv. Drug Deliv. Rev. 54:1145

19) Deming TJ (2005) Soft Matter 1:28

20) Yu M, Nowak AP, Pochan DJ Deming TJ (1999) J. Am. Chem. Soc. 121:12210

21) Hwang J, Deming TJ (2001) Biomacromolecules 2:17

22) Schaefer KE, Keller P, Deming TJ (2006) Macromolecules 39:19

23) Chen C, Wang Z, Li Z (2011) Biomacromolecules 12:2859

24) Kramer JR, Deming TJ (2010) J. Amer. Chem. Soc.132:15068

25) Kramer JR, Deming TJ (2012) J. Amer. Chem. Soc.134:4112

26) Liu Y, Chen P, Li Z (2012) Macromol. Rapid. Comm. 33:287

27) Kramer JR, Deming TJ (2010) Biomacromolecules 11:3668

28) Fu X, Shen Y, Fu W, Li Z (2013) Macromolecules 46:3753

29) Curtin SA, Deming TJ (1999) J. Am. Chem. Soc. 121:7427

30) Witte, P; Menzel, H (2004) Macromol. Chem. Phys. 205:1735

31) Sparks BJ, Ray JG, Savin, DA, Stafford CM, Patton DL (2011) Chem. Commun 47:6245

32) Rhodes AJ, Deming TJ (2012) J. Amer. Chem. Soc.134:19463

33) Brzezinska KR, Curtin SA, Deming TJ (2002) Macromolecules 35:2970

34) Cheng J, Deming TJ (1999) Macromolecules 32:4745

35) Seidel SW, Deming TJ (2003) Macromolecules 36:969

36) Goodwin AA, Bu X, Deming TJ (1999) J. Organometallic Chem. 589:111

37) Peng Y-L, Lai S-L Lin C-C (2008) Macromolecules 41:3455

38) Aliferis T, Iatrou H, Hadjichristidis N (2004) Biomacromolecules 5:1653

39) Mondeshki M, Spiess HW, Aliferis T, Iatrou H, Hadjichristidis N, Floudas G (2011) Eur. Polym. J. 47:668

40) Graf R, Spiess HW, Floudas G, Butt H.-J., Gkikas M, Iatrou H (2012) Macromolecules 45:9326

41) Thunig D, Semen J, Elias H-G (1977) Makromol. Chem. 178:603

42) Habraken GJM, Peeters M, Dietz CHJT, Koning CE, Heise A (2010) Polym. Chem. 1:514

43) Pickel DL, Politakos N, Avgeropoulos A, Messman JM (2009) Macromolecules 42:7781

44) Vayaboury W, Giani O, Cottet H, Deratani A, Schué F (2004) Macromol. Rapid Comm. 25:1221

45) Odian G (1991) Principles of Polymerization 3rd edn, Wiley, New York

46) Cao H, Yao J, Shao Z (2012) Polym. Int. 61:774

47) Nguyen L-TT, Vorenkamp EJ, Daumont CJM, ten Brinke G, Schouten AJ (2010) Polymer 51:1042

48) Habraken GJM, Wilsens KHRM, Koning CE, Heise A (2011) Polym. Chem. 2:1322

49) Dimitrov I, Schlaad H (2003) Chem. Commun. 2944

50) (a) Knobler Y, Bittner S, Frankel M (1964) J. Chem. Soc. 3941. (b) Knobler Y, Bittner S, Virov D, Frankel M (1969) J. Chem. Soc. (C) 1821

51) Meyer M, Schlaad H (2006) Macromolecules 39:3967

52) Lutz J-F, Schütt D, Kubowicz S (2005) Macromol. Rapid Commun. 26:23

53) Fischer H (2001) Chem Rev. 101:3581

54) Lu H, Cheng J (2007) J. Amer. Chem. Soc. 129:14114

55) Webster O (2000) J. Polym. Chem. Polym. Chem. Ed. 38:2855

56) Lu H, Cheng J (2008) J. Amer. Chem. Soc. 130:12562

57) Lu H, Wang J, Lin Y, Cheng J (2009) J. Amer. Chem. Soc. 131:13582

58) Uralil F, Hayashi T, Anderson JM, Hiltner A (1977) Polym. Eng. Sci. 17:515

59) Auer HE Doty P (1966) Biochemistry 5:1708

60) Ostroy SE, Lotan N, Ingwall RT, Scheraga HA (1970) Biopolymers 9:749

61) Epand RE, Scheraga HA (1968) Biopolymers 6:1551

62) Kubota S, Fasman GD (1975) Biopolymers 14:605

63) Cardinaux F, Howard JC, Taylor GT, Scheraga HA (1977) Biopolymers 16:2005

64) Ingwall RT, Scheraga HA Lotan N, Berger A, Katchalski E (1968) Biopolymers 6:331

65) Gibson MI, Cameron NR (2008) Angew. Chem. Int. Ed. 47:5160

66) (a) Nowak AP, Sato J, Breedveld V, Deming TJ (2006) Supramolecular Chemistry 18:423
(b) Li Z, Deming TJ (2010) Soft Matter 6:2546

67) Holt C, Horne DS (1996) Netherlands Milk and Dairy Journal 50:85

68) Alexandridis P, Holzwarth JF, Hatton TA (1994) Macromolecules 27:2414

69) Torchilin VP (2007) Phramaceutical Res. 24:1

70) Zhang LF, Eisenberg A (1995) Science 268:1728

71) Wilhelm, M, Zhao CL, Wang YC, Xu RL, Winnik MA, Mura JL, Riess G, Croucher MD (1991) Macromolecules 24:1033

72) Jeong YI, Cheon JB, Kim SH, Nah JW, Lee YM, Sung YK, Akaike T, Cho CS (1998) J. Controlled Rel. 51:169

73) Nah JW, Jeong YI, Cho CS (1998) Bull. Chem. Soc. Jpn. 19:962

74) Kwon G, Naito M, Yokoyama M, Okano T, Sakurai Y, Kataoka K (1993) Langmuir 9:945

75) Kidchob T, Kimura S, Imanishi Y (1998) J. Controlled Rel. 51:241

76) Hanson JA, Li Z, Deming TJ (2011) Macromolecules 43:6268

77) Hanson JA, Chang CB, Graves SM, Li Z, Mason TG, Deming TJ (2008) Nature 455:85

78) Hanson JA, Deming TJ (2011) Polym. Chem. 2:1473

79) Zhuang W, Liao L, Chen H, Wang J, Pan Y, Zhang L, Liu D (2009) Macromol. Rapid Commun. 30:920

80) Rutjes FPJT, van Hest JCM (2011) Polym. Chem. 2:1449

81) Bellomo E, Wyrsta MD, Pakstis L, Pochan DJ, Deming TJ (2004) Nature Materials 3:244

82) Rodriguez-Hernandez J, Lecommandoux S (2005) J. Amer. Chem. Soc. 2127:2026

83) Sela M, Katchalski E (1959) Adv. Protein Chem. 14:391

84) Holowka EP, Pochan DJ, Deming TJ (2005) J. Amer. Chem. Soc. 127:12423

85) Nowak AP, Breedveld V, Pakstis L, Ozbas B, Pine DJ, Pochan D, Deming TJ (2002) Nature 417:424

86) Choe U-J, Rodriguez AR, Lee BS, Knowles SM, Wu AM, Deming TJ, Kamei DT (2013) Biomacromolecules 14:1458

87) Holowka EP, Sun VZ, Kamei DT, Deming TJ (2007) Nature Mater. 6:52

88) Sun VZ, Li Z, Deming TJ, Kamei DT (2011) Biomacromolecules 12:10

89) Sun VZ, Choe U-J, Rodriguez AR, Dai H, Deming TJ, Kamei DT (2013) Biomacromolecules 13:539

90) Iatrou H, Frielinghaus H, Hanski S, Ferderigos N, Ruokolainen J, Ikkala O, Richter D, Mays J, Hadjichristidis N (2007) Biomacromolecules 8:2173

91) Sun J, Huang Y, Shi Q, Chen X, Jing X (2009) Langmuir 25:13726

92) Rodriguez AR, Choe U-J, Kamei DT, Deming TJ (2012) Macromol. Biosci. 12:805

93) Gaspard J, Silas JA, Shantz DF, Jan J-S (2010) Supramolecular Chem. 22:178

94) Lai J-K, Chuang T-H, Jan J-S, Wang SS-S (2010) Coll. Surf. B: Biointerfaces 80:51

95) Holowka EP, Deming TJ (2010) Macromol. Biosci. 10:496

96) Waite J H. (1992) Biol. Bull. 183:178

97) Sulistio A, Blencowe A, Wang J, Bryant G, Zhang X, Qiao GG (2012) Macromol. Biosci. 12:1220

98) Huang J, Bonduelle C, Thévenot J, Lecommandoux S, Heise A (2012) J. Amer. Chem. Soc. 134:119

99) Kramer JR, Rodriguez AR, Choe U-J, Kamei DT, Deming TJ (2013) Soft Matter 9:3389

100) Lee KY, Mooney DJ (2001) Chemical Reviews 101:1869

101) Peppas NA, Huang Y, Torres-Lugo M, Ward JH, Zhang J (2000) Annual Review of Biomedical Engineering, 2:9

102) Lutolf MP, Hubbell JA (2005) Nature Biotech. 23:47

103) Zisch AH, Lutolf MP, Hubbell JA (2003) Cardiovascular Pathology 12:295

104) Pakstis L, Ozbas B, Nowak AP, Deming TJ, Pochan DJ (2004) Biomacromolecules 5:312

105) Aggeli A, Nyrkova IA, Bell M, Harding R, Carrick L, McLeish,TCB, Semenov AN, Boden N (2001) Proc. Natl. Acad. Sci. (USA) 98:11857

106) Nowak AP, Breedveld V, Pine DJ, Deming TJ (2003) J. Amer. Chem. Soc. 125:15666

107) Richert L, Lavalle P, Vautier D, Senger B, Stoltz JF, Schaaf P, Voegel JC, Picart C (2002) Biomacromolecules 3:1170

108) Aggeli A, Bell M, Boden N, Keen JN, Knowles PF, McLeish TCB, Pitkeathly M, Radford SE (1997) Nature 386:259

109) Zhang S, Marini DN, Hwang W, Santoso S (2002) Curr. Opn. Chem. Biol. 6:865

110) Tanaka T (1981) Scientific American 244:124

111) Hu Y-Y, Yusufoglu Y, Kanapathipillai M, Yang C-Y, Wu Y, Thiyagarajan P, Deming TJ, Akinc M, Schmidt-Rohr K, Mallapragada S, (209) Soft Matter 5:4311

112) Xia L, Liu Y, Li Z (2010) Macromol. Biosci. 10:1566

113) Katchalski E, Sela MB (1958) Adv. Protein Chem. 13:243

114) Yang C-Y, Song B, Ao Y, Nowak AP, Abelowitz RB, Korsak RA, Havton LA, Deming TJ, Sofroniew MV (2009) Biomaterials 30:2881

115) Song B, Song J, Zhang S, Anderson MA, Ao Y, Yang C-Y, Deming TJ, Sofroniew MV (2012) Biomaterials 33:9105

Equations

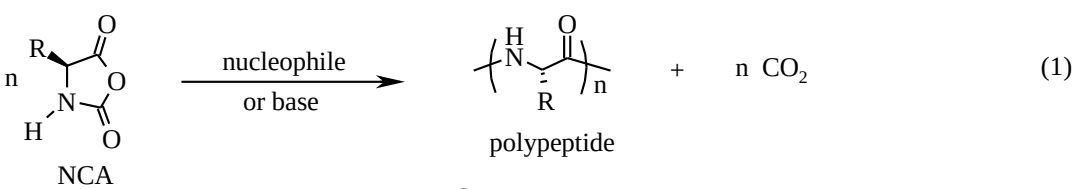

(1)

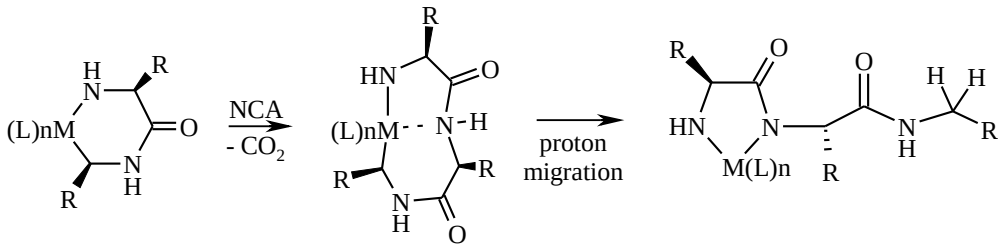

(5)

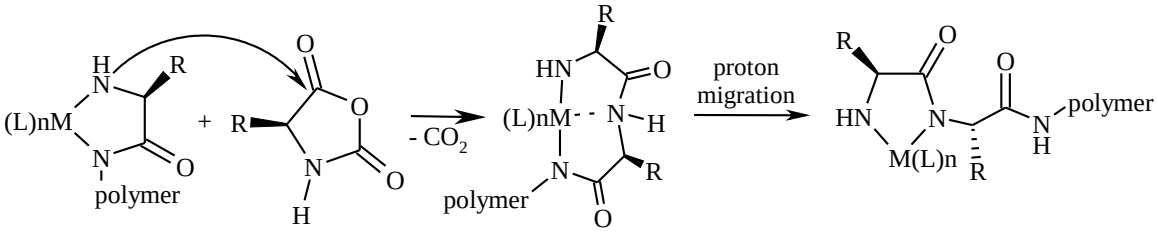

(6)

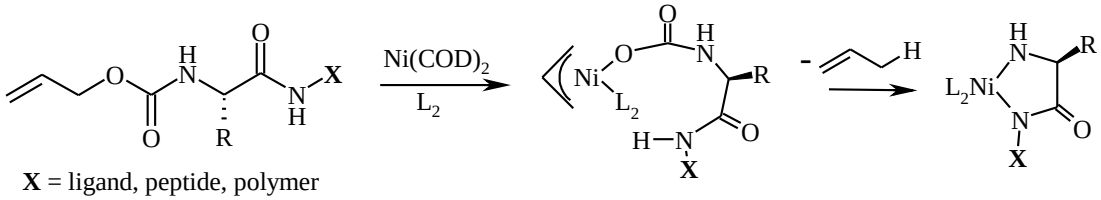

X = ligand, peptide, polymer

(7)

(8)

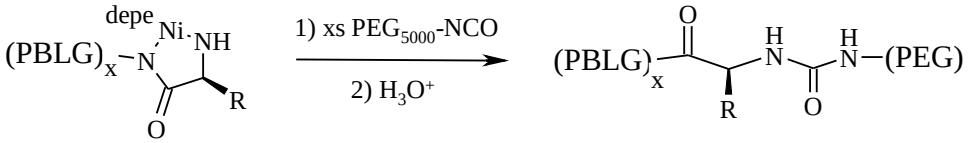

(9)

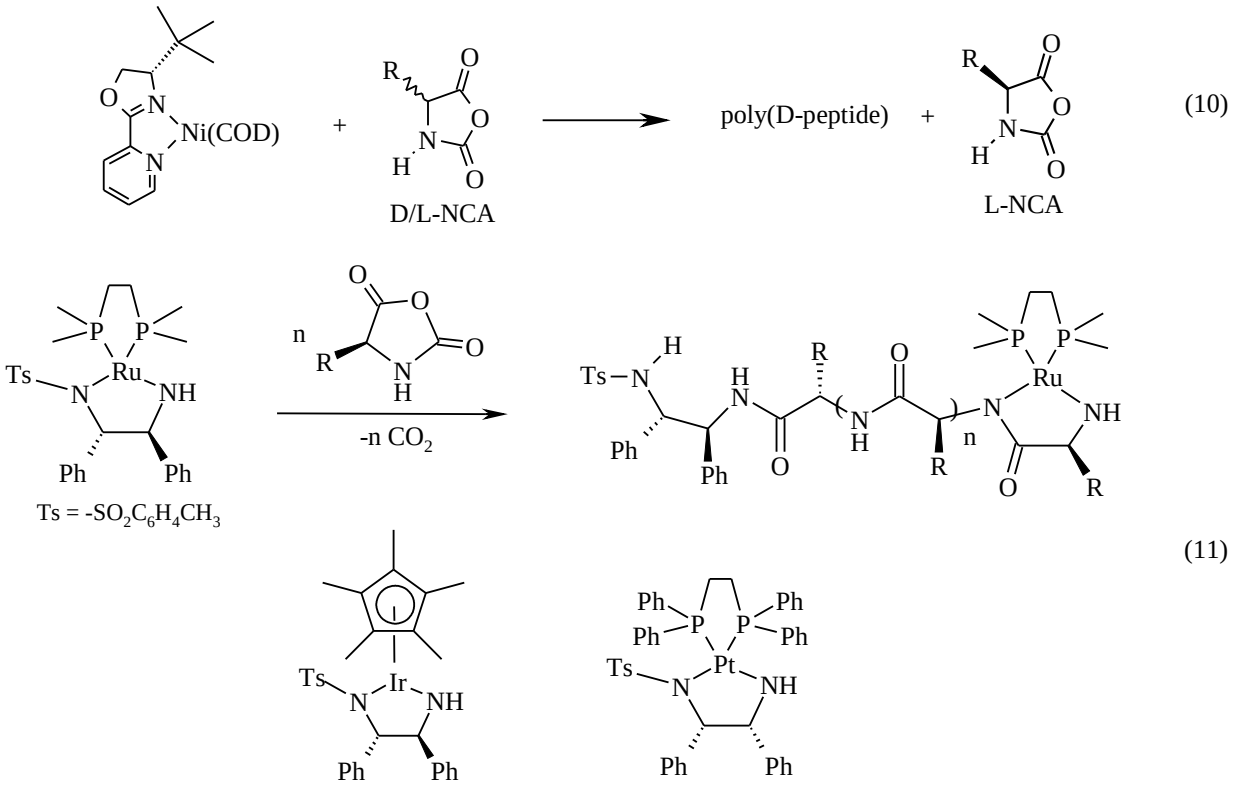
Ni(COD)
D/L-NCA
poly(D-peptide)
L-NCA
Ts = -SO2C6H4CH3
-n CO2
Ir
Pt

(10)

(11)

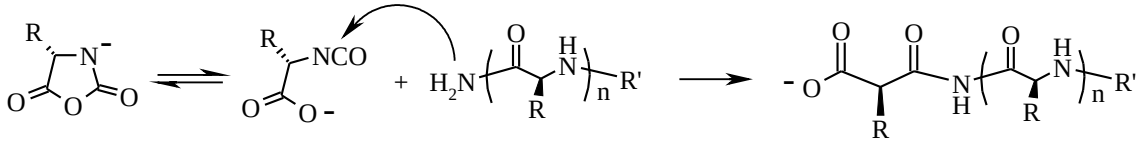

(12)

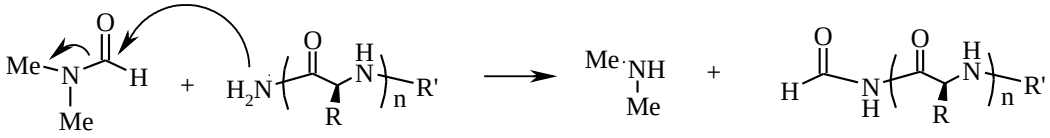

(13)

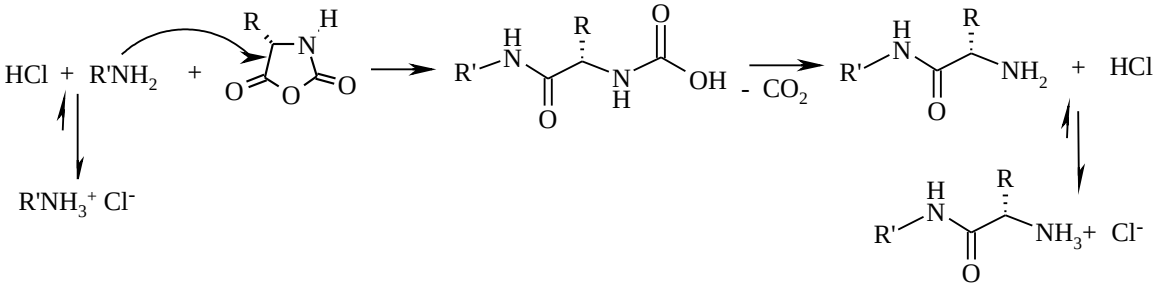
HCl + R'NH2
R'NH3+ Cl-
- CO2
HCl
R'NH3+ Cl-

(14)

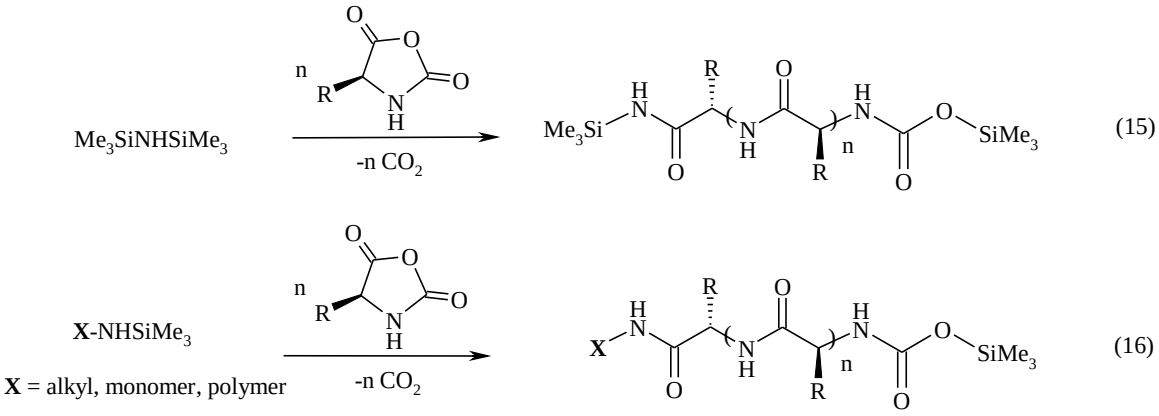
Me3SiNHSiMe3
-n CO2
Me3Si
SiMe3

(15)

X-NHSiMe3
X = alkyl, monomer, polymer
-n CO2
X
SiMe3

(16)

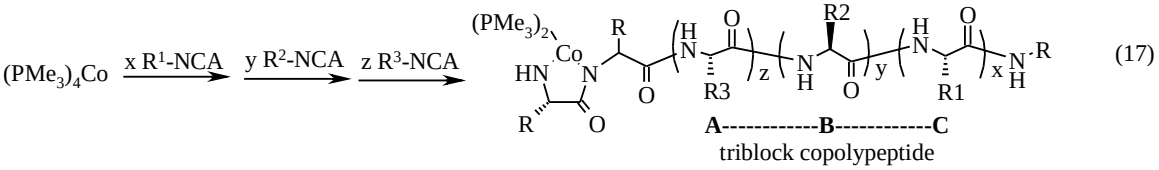
(PMe3)4Co
x R1-NCA
y R2-NCA
z R3-NCA
(PMe3)2
A----------B----------C
triblock copolypeptide

(17)

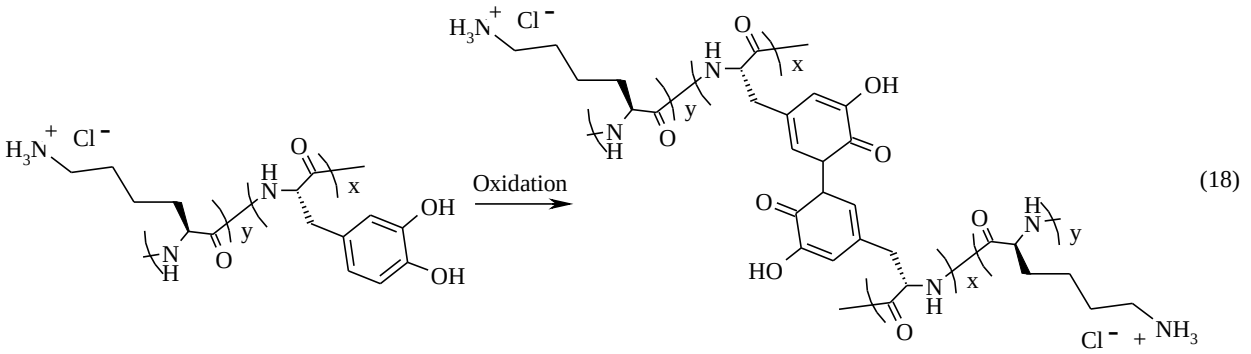
Oxidation
Cl -
NH3

(18)

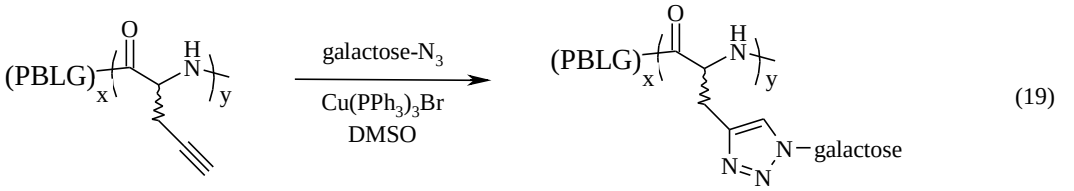
(PBLG)
galactose-N3
Cu(PPh3)3Br
DMSO
galactose

(19)

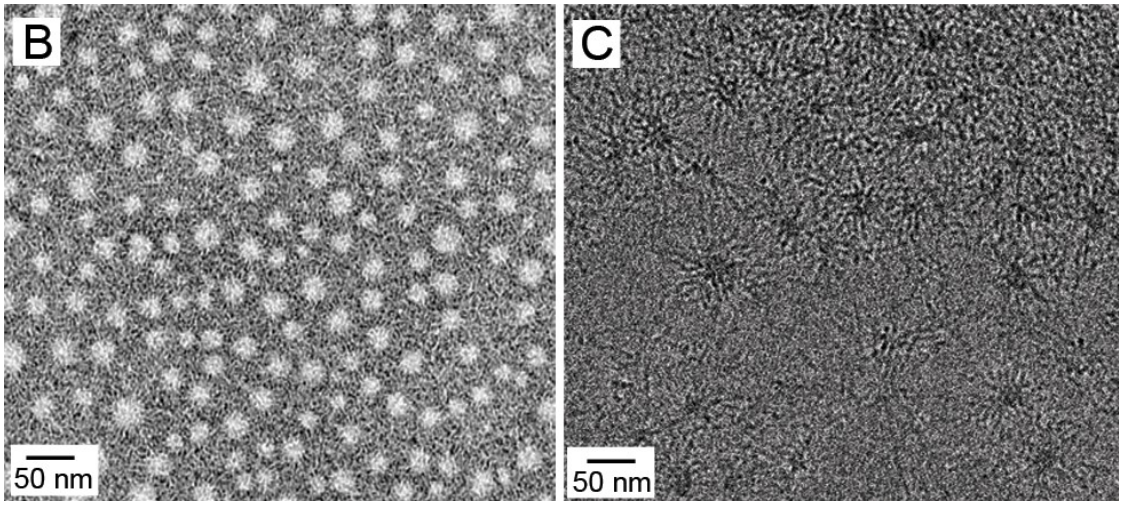

Figure 1 A) Schematic showing $K^{P}_{x}(rac\text{-}L)_{y}$ block copolypeptides and self-assembly into micelles. B) Negative stain TEM image showing nanostructure of $K^{P}_{100}(rac\text{-}L)_{10}$ micelles. C)

Cryogenic TEM image of a 0.50 % (w/v) aqueous suspension of K^{P}_{100}(*rac*-L)$_{10}$. Scale bars = 50 nm. Adapted from [76].

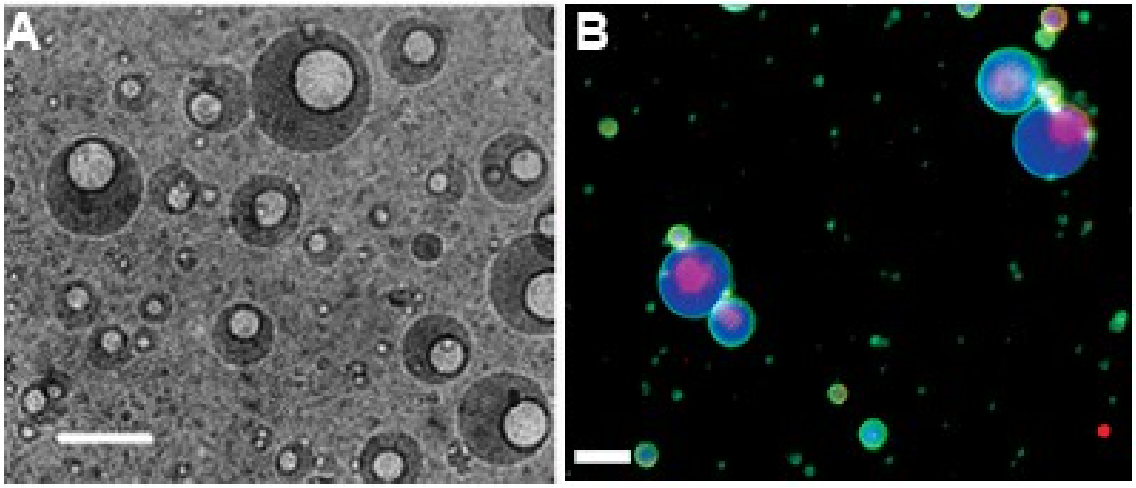

Figure 2 A) Cryogenic TEM image size-fractionated K_{40}(*rac*-L)$_{20}$ double emulsions (bar = 70 nm). B) FITC-labeled K_{40}(*rac*-L)$_{10}$ (green) double emulsion loaded with both pyrene (blue) and InGaP quantum dots (red) (bar = 5 μm). Adapted from [77].

A **B**

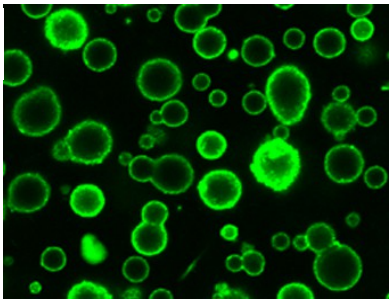

Figure 3 Non-ionic polypeptide

C

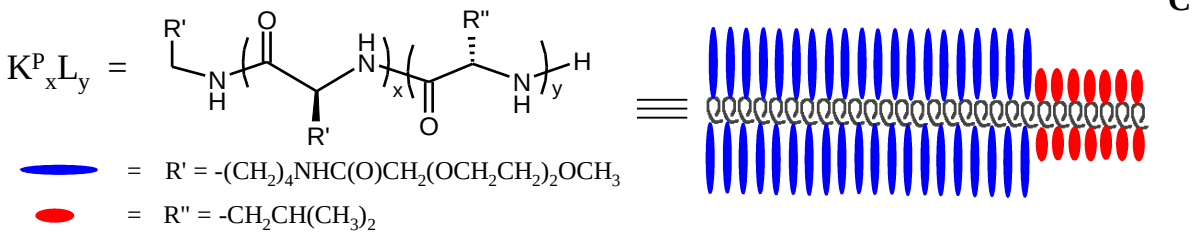

vesicles. A) LSCM image (50 μm wide) of a $K^{P}_{100}L_{20}$ vesicle suspension visualized with fluorescent probes and a Z-direction slice thickness of 490 nm. B) Drawing illustrating proposed packing of $K^{P}_{x}L_{y}$ chains in vesicle walls. C) Structure and cartoon of $K^{P}_{x}L_{y}$ chains. Adapted from [81].

Figure 4 A and B) DIC images of 1 % (w/v) polypeptide vesicles extruded through 1.0 μm PC filters (Bars = 5 μm). **A** = $K_{60}L_{20}$ and **B** = $E_{60}L_{20}$. C) Negative stained TEM image of 0.1 % (w/v) $K_{60}L_{20}$ 0.1 μm filtered vesicles (Bar = 350 nm). D) Average diameter (from DLS) of 1 % (w/v)

$K_{60}L_{20}$ (filled circles) and $E_{60}L_{20}$ (open diamonds) vesicles versus PC filter size. Adapted from [84].

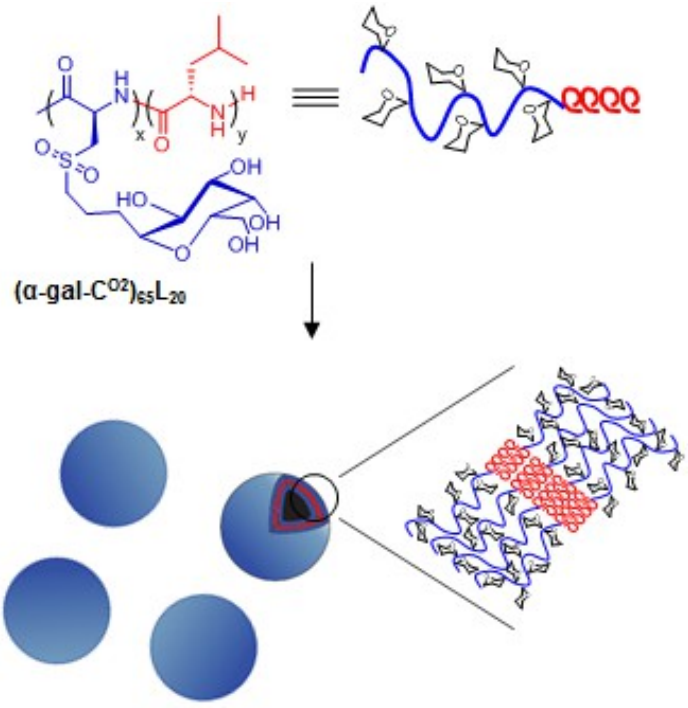

Figure 5. Schematic showing structures of amphiphilic glycosylated diblock copolypeptides and their assembly into vesicles. Adapted from [99].

A

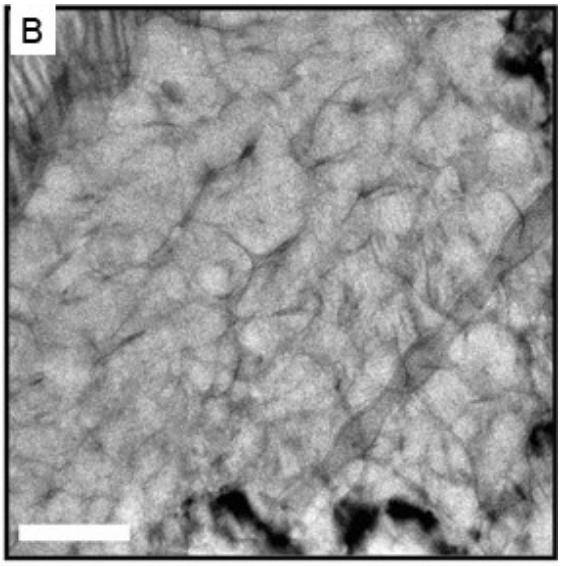
B

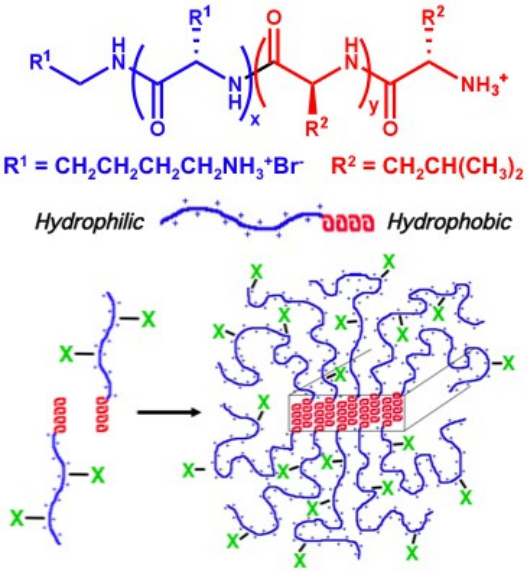
R1 = CH2CH2CH2CH2NH3+Br-
R2 = CH2CH(CH3)2
Hydrophilic
Hydrophobic

Figure 6 A) Schematic representations of block copolypeptide hydrogel composition and structure. Block copolypeptides are composed of variable-length chains of hydrophilic (blue) and hydrophobic (red) amino acids. In aqueous solution, hydrophobic segments associate into elongated fibrillar assemblies that entangle to form 3D networks with hydrophilic segments exposed. B) Cryogenic TEM image of vitrified $K_{180}L_{30}$ hydrogel. Bar = 200 nm.

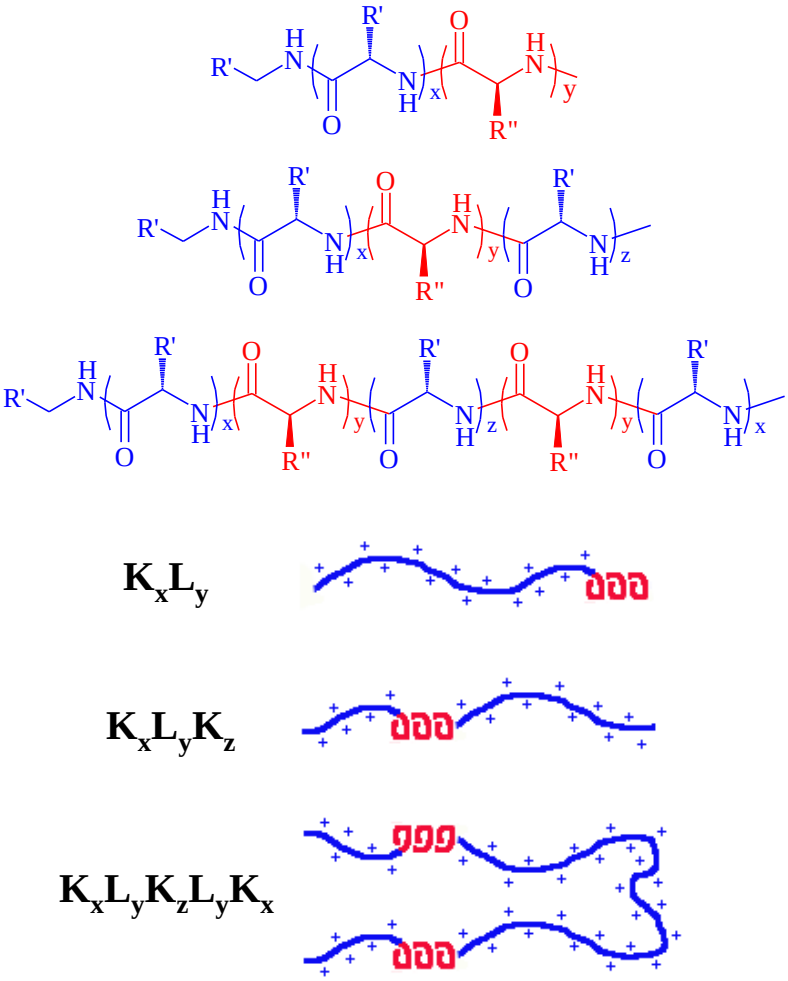

Figure 7 Structures and schematic illustrations of diblock, triblock and pentablock copolypeptides. R' = $-CH_2CH_2CH_2CH_2NH_3^+Br^-$ and R" = $-CH_2CH(CH_3)_2$. Adapted from [66].

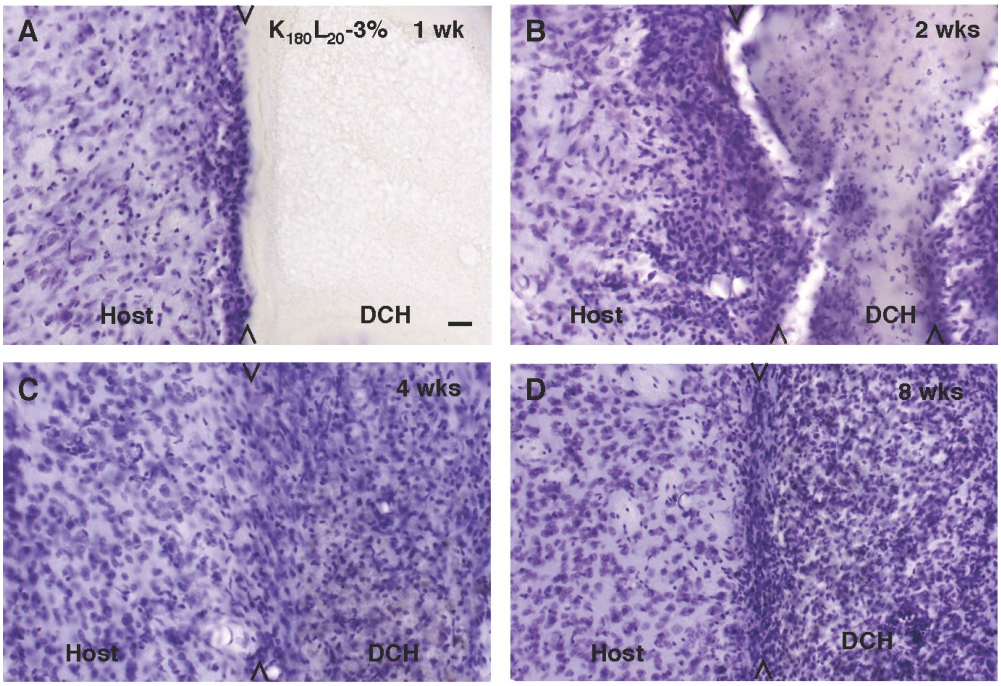

Figure 8 Time-dependent migration of cells into block copolypeptide hydrogel deposits in vivo. A–D) Light-microscopic images of 3% $K_{180}L_{20}$ at 1 (A), 2 (B), 4 (C) and 8 (D) weeks after injection of 2 µl into the striatum in cresyl violet stained tissue sections. Essentially no cells are present in the deposits after 1 week in vivo (A). After 2 weeks in vivo (B), a number of cells have migrated into, and are scattered throughout the deposits and after 4 (C) and 8 weeks (D) the deposits are densely packed with cells. Arrowheads indicate the borders of deposit and host tissue. Scale bar: A–D = 25 mm. Adapted from [114].

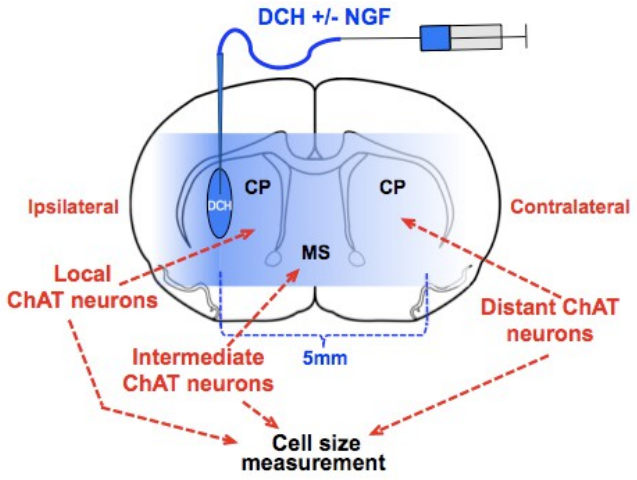

A B

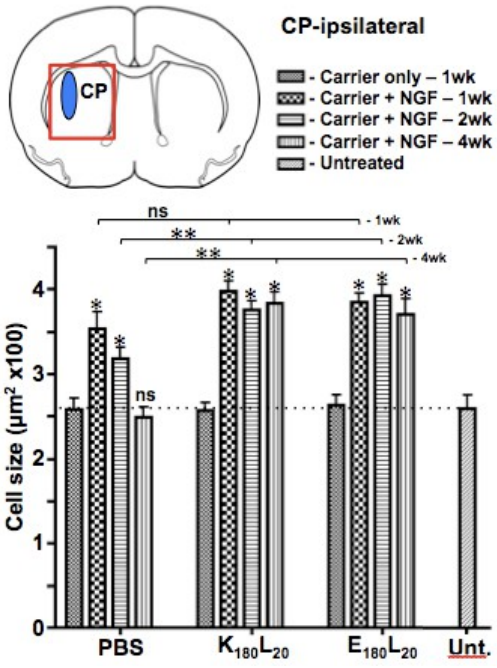

Figure 9 A) Schematic of experimental design to evaluate release of NGF from $K_{180}L_{20}$ hydrogel (DCH) depots in vivo. NGF is known to induce hypertrophy of basal forebrain cholinergic (ChAT) neurons in the caudate putamen (CP) and medial septum (MS). Depots of DCH with NGF were injected into the CP on one side of the brain. B) Effects of NGF released from DCH depots on local forebrain cholinergic neurons in ipsilateral caudate putamen. Box in schematic drawing outlines the location of cholinergic neurons evaluated in the ipsilateral CP local to the DCH depot. Graph shows mean cell area in mm^2 of cholinergic neurons in various treatment groups and at various treatment times as indicated. n = 4 per group, *p < 0.01 relative to carrier only, **p < 0.01 for group comparisons as indicated, ns non-significant, ANOVA with Newman-Keuls post-hoc pair-wise comparisons. Adapted from [115].

Graphical Abstract: